The Effects of Atmosphere-Ocean Climate Oscillations on and Trends in Saskatchewan River Discharges

Jeannine-Marie St. Jacques, Yuhui Althea Huang, Yang Zhao, Suzan L. Lapp and David J. Sauchyn

Prepared for the Saskatchewan Watershed Authority

April 1, 2011

Summary

Canadian western interior precipitation and temperature are heavily influenced by recurring large-scale climate patterns: the Pacific Decadal Oscillation (PDO), the El Niño-Southern Oscillation (ENSO), the Pacific North American mode (PNA) and the Arctic Oscillation (AO). We examined relationships between Saskatchewan streamflow and these low frequency atmospheric and oceanic climate oscillations: the PDO, ENSO, PNA and AO. Twenty-six naturally-flowing stream discharge records geographically distributed across the province were analyzed using composite analyses based upon Monte Carlo permutation *t*-tests. These composite analyses demonstrated that the PDO and PNA have a clear impact on Saskatchewan annual mean daily discharge, with higher annual discharges occurring during negative PDO and negative PNA years, and lower flows during the positive phase years throughout most of the province. Composite analyses also show the impact of ENSO, and the weaker affect of the AO, again with higher flows during La Niña and the negative AO years, and lower flows during El Niño and the positive AO years throughout most of the province. The phase relationship is reversed in the very far north, where discharges are higher during the positive PDO, positive PNA, El Niño and positive AO years, and lower during the negative phase years. Patterns of streamflow variation according to climate oscillation phases closely follow the patterns of precipitation variation according to climate oscillation phases. The probability of two successive years of least quartile flows in the South Saskatchewan River Basin is much greater in the positive PDO phase, and nearly zero in the negative PDO phase. Conversely, the probability of two successive years of highest quartile flows in the South Saskatchewan River Basin is much greater in the negative PDO phase, and much smaller in the positive PDO phase.

The detection and attribution of past trends and variability in hydrological variables is essential for the understanding of future climate change and prudent water management in a semi-arid climate such as that of southern Saskatchewan. Because trend analyses of Saskatchewan river annual discharges are either not based upon recent data (*e.g*., *Westmacott and Burn*, 1997; *Yulianti and Burn*, 1998; *Gan*, 1998; *Zhang et al*., 2001) and/or do not deal with the problem of autocorrelation biasing the trend test according to the most recent best practice (*Burn et al.*, 2008; *Khaliq et al*., 2009), we examined 26 naturally-flowing annual mean daily flow records and 10 regulated river records from through-out Saskatchewan and environs for trends using a modified Mann-Kendall test. There is a decline in annual mean daily flow in the naturally-flowing streams in the southwest corner of the province. There also are significant declines in the regulated flows of the South Saskatchewan River Basin, which propagates all the way downstream to the gauge at Le Pas, Manitoba, which shows a highly significant decline over its entire period of record. Apart from the southwest corner, annual naturally-flowing hydrological series through-out the rest of the province show no significant trends when tested over their entire period of record.

Part I. Atmosphere-Ocean Climate Oscillations Effects on Saskatchewan River Discharges

Introduction

Canadian western interior climatology is heavily influenced by recurring large-scale climate patterns: the Pacific Decadal Oscillation (PDO), the El Niño-Southern Oscillation (ENSO), the Pacific North American mode (PNA) and the Arctic Oscillation (AO). The Canadian Western Interior hydroclimate, like that of much of western North America, displays strong periodic cycles linked to the low-frequency Pacific Decadal Oscillation (PDO) (*Mantua et al.*, 1997; *Stewart et al*., 2005; *St. Jacques et al.*, 2010). The PDO is a pattern of climate variability that shifts phases on an inter-decadal time scale, usually about 20 to 35 years (*Minobe* 1997; *Mantua and Hare*, 2002). In 1890, the PDO entered into a predominately cool (negative) phase, which continued until 1925 when a warm (positive) phase began. In 1947, the PDO shifted back into a cool phase, which lasted until 1977, whereupon a warm phase began. Winter precipitation in the northern Rocky Mountains is higher when the PDO is in a negative phase (*Mantua et al.*, 1997; *Comeau et al*., 2009; *Wise*, 2010). A strong negative relationship exists between the PDO and precipitation and streamflow in south and central Alberta, British Columbia and Montana; therefore, these regions are wetter when the PDO is in its negative phase and drier when the PDO is positive (Figure 2). The higher frequency ENSO also affects the hydroclimatology of this region as precipitation and streamflow are decreased during El Niño events and increased during La Niña events (*Shabbar and Khandekar*, 1996; *Shabbar et al*., 1997; *Bonsal and Lawford*, 1999; *Bonsal et al*., 2001; *Shabbar and Skinner,* 2004; *Bonsal and Shabbar*, 2008) (Figure 3). The Pacific North American mode (PNA) is one of the most prominent modes of low-frequency atmospheric variability in the Northern Hemisphere extratropics (*Wallace and Gutzler*, 1981). The PNA pattern is associated with strong fluctuations in the strength and location of the East Asian jet stream. The positive phase of the PNA pattern is associated with above-average temperatures over western Canada and above-average precipitation anomalies in the Gulf of Alaska, extending into the Pacific Northwest (Figure 4). The Arctic Oscillation (AO) is a measure of the intensity of the polar vortex and is closely related to (if not the same as) the North Atlantic Oscillation (NAO) (*Wallace and Gutzler*, 1981). A negative relationship exists between northern Prairie winter precipitation and the NAO, as the positive NAO (and AO) allows more frequent outbreaks of cold, dry Arctic air to this region (Figure 5) (*Bonsal and Shabbar*, 2008; their Figure 3).

The hydroclimatology of British Columbia and Alberta has been well-studied recently (e.g., *Stewart et al*., 2005; *Gobena and Gan*, 2006; *St. Jacques et al.*, 2010), but that of Saskatchewan and Manitoba much less so (*e.g*., *Gan*, 1998; *Zhang et al*., 2001; *Burn et al*., 2008). In this section, we examine relationships between Saskatchewan streamflow and these low frequency atmospheric and oceanic climate oscillations: the PDO, ENSO, PNA and AO.

Datasets and methods

Because human impact obscures the natural hydroclimatology, for this portion of our study, we only analyzed naturally-flowing streams and rivers. We tried to analyze the two longest continuous river discharge records in each drainage sub-basin, thus giving a reasonable geographical coverage of Saskatchewan. Unfortunately, this was not always possible due to lack of gauges, particularly in the north. In total, 26 stream discharge records were analyzed; all had active gauges (Table 1). Mean daily flows averaged over the year or March-October (many of the gauges on the smaller streams are not recording in winter) were used. In the heavily human modified landscape of South Saskatchewan, the only naturally flowing rivers are relatively small, with mean daily flow less than 5.0 m^3/s and drainage area less than 2,600 km^2 (Table 1). These small southern streams have high coefficients of variation, as their flows can change dramatically from year to year (Table 2). In the relatively unpopulated northern half of the province, the naturally flowing rivers are relatively large, with mean daily flow greater than 15.0 m^3/s and effective drainage area greater than 3,000 km^2 (Table 1). Typically, coefficients of variation for the northern rivers are much lower, as year to year flows are steadier. Shapiro-Wilk tests demonstrated that most records were not normally distributed, particularly for the smaller streams (Table 2). Our choice of method of statistical analysis was greatly constrained by the shortness of record length, as continuous records only begin in the 1970s for nine rivers and in the 1960s for another nine rivers. We extracted the streamflow records from the Water Survey of Canada (HYDAT) (http://www.wsc.ec.gc.ca/) database, augmented by internal data from Saskatchewan Watershed Authority (courtesy of Jeremy Pitman) (Figure 1 and Table 1).

The sea surface temperature-based (SST) monthly PDO time series of *Mantua et al*. (1997) and *Zhang et al*. (1997) was obtained from the Joint Institute for the Study of the Atmosphere and Ocean (http://jisao.washington.edu/pdo/). There are a multitude of ENSO metrics available (http://www.cdc.noaa.gov/ClimateIndices/); however, only one starts by 1900, the sea level pressure-based (SLP) monthly Southern Oscillation Index (SOI) (*i.e*., the normalized difference between monthly mean SLP at Tahiti, French Polynesia and Darwin, Australia) (*Ropelewski and Jones*, 1987). A few of the Saskatchewan streamflow gauges have data beginning in the 1910s and 1920s, such as Rock and Lyons Creeks, and we wished to incorporate these data into the study. The SOI and the 500 millibar height-based monthly PNA were obtained from Earth Systems Research Laboratory (National Oceanic and Atmospheric Administration, 2009, http://www.cdc.noaa.gov/ClimateIndices/). The SLP-based December-March averaged AO index was obtained from James Hurrell at the National Center for Atmospheric Research (http://www.cgd.ucar.edu/cas/jhurrell/indices.html) (also called the Northern Annular Mode or NAM). (Figure 6) All time series began by 1900, except for the PNA, which commenced by 1950, the year upper atmospheric data became dense enough to produce world-wide coverage.

The relationships between streamflow and the climate oscillations were examined by composite analysis, as the shortness of the discharge records (typically of length less than one ~60-year PDO cycle), and the typical non-normality of the records precluded using a parametric method such as generalized least squares regression. For each climate oscillation and for each Saskatchewan river, mean daily discharges are composited into two classes: those corresponding to the strong positive climate oscillation events and those corresponding to the strong negative climate oscillation events. The differences in average discharge between the two classes were then assessed using a Monte Carlo permutation *t*-test (see appendix for sample R code). A permutation *t*-test, rather than a regular classical *t*-test was required because of the typical extreme non-normality of the mean daily discharges (*Manly*, 1998).

For the composite analyses, individual strong positive and negative climate oscillation events are required. Strong positive PDO events are defined as those years in which the winter averaged (November-March) PDO was greater or equal to 0.75 standard deviations from the mean; and, correspondingly, strong negative PDO events are defined as those years in which the winter averaged PDO was less than or equal to -0.75 standard deviations (Table 3). Strong positive PNA events are defined as those years in which the winter averaged (December-February) PNA was greater or equal to 0.75 standard deviations from the mean; whereas strong negative PNA events are defined as those years in which the winter averaged PNA was less than or equal to -0.75 standard deviations (Table 3). Strong positive AO events are defined as those years in which the winter averaged (December-March) AO was greater or equal to 0.80 standard deviations from the mean; strong negative AO events are defined as those years in which the winter averaged AO was less than or equal to -0.80 standard deviations (Table 3). The winter values of the PDO, PNA and AO are used because the oscillations are strongest in winter, and their downstream teleconnections are strongly correlated to Saskatchewan winter precipitation (Figures 2, 4 and 5). Winter snowfall is the source of much of the water flowing in the local rivers (*Pham et al.*, 2009). Even if the season of analysis started in November or December, the season was assigned the year date corresponding to January, *i.e.*, a strong negative PDO event during November and December 2007, and continuing January through March 2008, was assigned the year 2008; and similarly for the PNA and AO. It would have been statistically preferable to define events in terms of ± 1.0 standard deviations from the mean. However, since so many Saskatchewan streamflow records began in the 1970s, this definition would have resulted in too few negative phase PDO, PNA and AO events for subsequent analysis (a minimum of four such events are needed for the Monte Carlo tests). Neutral years for a climate oscillation refer to years that are marked by neither a strong positive or strong negative climate oscillation event.

The SOI was handled differently. Strong or moderate El Niño events were defined as when the averaged June-November SOI < -0.5, and a La Niña event was when the averaged June-November SOI > 0.5 (Table 3), following *Redmond and Koch* (1991). These authors found better correlations between the SOI and Pacific Northwest winter climate when the SOI leads by a few months, as the teleconnection between the tropical Pacific Ocean and the downstream Pacific Northwest operates at a definite multi-monthly lag. Therefore, we maintained this relationship by comparing the leading SOI (June-November) event to the following year's streamflow (January-December, or March-October), as it is the immediate winter after an El Niño or La Niña event that is drier or wetter on the Prairies (Figure 3) (*Shabbar et al.*, 1997; *Bonsal and Shabbar*, 2008; their Figure 2).

Both two-sample and one-sample permutation *t*-tests were performed for each of the four climate oscillations and for each individual streamflow magnitude time series of length *n*. In the two-sample *t*-tests, the n_1 streamflow magnitudes corresponding to the positive climate oscillation events were compared to the n_2 streamflow magnitudes corresponding to the negative climate oscillation events, and a regular a *t*-statistic between the two was computed (add equation). Then, the merged $n_1 + n_2$ streamflow magnitudes time series corresponding to both strong phases of the climate oscillation was randomly shuffled and divided into an n_1 initial portion and an n_2 latter portion, and a *t*-statistic between the two was computed (*R Development Core Team*, 2008). This was done 10,000 times. The number of times the actual *t*-statistic exceeded the randomly simulated *t*-statistic was determined, as was the number of times the converse occurred, and the one-tailed significance was assessed at the 10% level, which is typically used in geophysical data. In the one-sample *t*-tests, the n_1 (n_2) streamflow magnitudes corresponding to the positive (negative) climate oscillation events were compared to all the n-n_1 (n-n_2) remaining streamflow magnitudes corresponding to both the negative (positive) and neutral climate oscillation events, and a regular a *t*-statistic between the two was computed, and the permutations were done analoguously. One-sample *t*-tests were performed in case the effect of the climate oscillation is asymmetric in any given watershed. One-tailed *t*-tests are reasonable because there is evidence justifying choice of tail from correlation analysis between winter precipitation and the climate oscillations (Figures 2, 3, 4 and 5). For example, when a significant negative correlation exists between winter precipitation falling on a watershed and the PDO, we expect the appropriate one-sided result from the permutation *t*-test between streamflow magnitude at a gauge in that watershed and the PDO.

Because it is known that the PDO has a large effect on winter prairie precipitation and the immediate subsequent year streamflow (*e.g.*, *Mantua et al.*, 1997; *Mantua and Hare*, 2002; *Whitfield et al*., 2010; *St. Jacques et al.*, 2010), we examined the effect of PDO phase on the probability of two years of successive low or high flows of Saskatchewan River tributaries. The reservoir capacity of the Alberta portion of the North and South Saskatchewan Rivers basins is estimated to be two years in case of drought (*personal comm., Michael Seneka, Alberta Environment*); hence, the interest in two successive years of low annual discharge. Twenty-five of the longest (centennial-scale length), most continuous mean daily flows (annualized) of Saskatchewan River tributaries or neighboring rivers were examined from the headwaters in Alberta and downstream (Table 4). Both actual and naturalized flows were included. Details of 23 of the records are described in *St. Jacques et al.* (2010); the other two gauges are the North Saskatchewan River at Prince Albert and the Saskatchewan River at Le Pas, Manitoba. The PDO was in a warm phase from 1925-1946 and 1977-2007, in a cool phase from 1900-1924 and 1947-1976. For each gauge, the mean daily flow magnitudes were ranked into quartiles. The number of two successive years of least quartile streamflows were tallied and examined according to PDO phase. The probability of two successive years of least quartile flow in a given PDO phase is estimated by the number of two successive years of least quartile streamflows strictly occurring in that phase divided by the total number of two successive years occurring in that phase with streamflow data. The analogous estimation was made for the highest quartile flow probabilities.

Results

A clear, strong fingerprint of the extra-tropical oceanic PDO is shown on Saskatchewan naturally-flowing mean river discharges (Table A1 and Figure 7a). Fifteen of the 26 gauge records (58%) had a significant permutation *t*-test (at the *0.10* significance level), with a predominance of the significant *t*-tests being either two-sample tests or tests of streamflow magnitudes occurring during strong positive PDO events against the remaining streamflow magnitudes. The signs of the significant *t*-tests followed the geographical pattern predicted by the correlation map between the winter PDO and concurrent precipitation (Figure 2): a negative relationship between the PDO and streamflow through-out the province except for the northeast corner where the relationship becomes positive for the Fond du Lac gauge (Table A1 and Figure 7a).

A strong fingerprint of the tropical atmospheric SOI is shown on Saskatchewan naturally-flowing mean river discharges (Table A2 and Figure 7b). Thirteen of the 26 gauge records (50%) had a significant permutation *t*-test (at the *0.10* significance level), with a predominance of the significant *t*-tests being either two-sample tests or tests of streamflow magnitudes occurring during strong positive SOI (La Niña) events against the remaining streamflow magnitudes. The signs of the significant *t*-tests followed the geographical pattern predicted by the correlation map between the SOI and precipitation (Figure 3): a positive relationship between the SOI and streamflow through-out the province except for the northeast corner where the relationship becomes negative for the MacFarlane gauge (Table A2 and Figure 7b). The negative relationship at the Maloneck Creek gauge may be anomalous.

A clear, strong fingerprint of the extra-tropical atmospheric PNA is also shown on Saskatchewan naturally-flowing mean river discharges (Table A3 and Figure 7c). Fifteen of the 26 (58%) gauge records had a significant permutation *t*-test (at the *0.10* significance level), with a predominance of the significant *t*-tests being either two-sample tests or tests of streamflow magnitudes occurring during strong positive PNA events against the remaining streamflow magnitudes. The signs of the significant *t*-tests followed the geographical pattern predicted by the correlation map between the winter PNA and concurrent precipitation (Figure 4): a negative relationship between the PNA and streamflow through-out the province except for the far north where the relationship becomes positive for the Fond du Lac and MacFarlane gauges (Table A3 and Figure 7c). Associated *p*-levels of the significant *t*-tests were particularly small, demonstrating how unlikely it is for these relationships to occur by chance.

A weaker fingerprint of the polar atmospheric AO is also shown on Saskatchewan naturally-flowing mean river discharges (Table A4 and Figure 7d). Ten of the 26 gauge records (38%) had a significant permutation *t*-test (at the *0.10* significance level). The signs of the significant *t*-tests followed the geographical pattern predicted by the correlation map between the winter NAO (used a proxy for the nearly identical AO) and concurrent precipitation (Figure 5): a negative relationship between the AO and streamflow in the southern half of the province, except in the far north where the relationship becomes significantly positive for the Fond du Lac gauge (Table A4 and Figure 7d).

There is a definite asymmetry in the effect of PDO phase on the probability of two years of successive least (or highest) quartile flows of Saskatchewan River tributaries (Table 4). The mean probability of two years of successive least quartile flows is 0.149 during the positive phase of the PDO; this probability drops to a negligible 0.015 during the negative phase of the PDO. Conversely, the mean probability of two years of successive highest quartile flows is a small 0.043 during the positive phase of the PDO; this probability increases to 0.135 during the negative phase of the PDO. This pattern in the low quartile flows is seen at 24 of the examined discharge records; the Red Deer River at Red Deer is the exception. This pattern in the high quartile flows is seen at 23 of the examined discharge records; the Bow River at Banff and the Columbia River at Nicholson are the exceptions.

Discussion

Composite analyses based upon Monte Carlo permutation *t*-tests show that the PDO and the PNA have a clear impact on Saskatchewan annual mean daily discharge, with higher annual discharges occurring during negative PDO and negative PNA years, and lower flows during the positive phase years throughout most of the province (Figure 7, Tables A1 and A3). Composite analyses also show the impact of ENSO, and the weaker affect of the AO, again with higher flows during La Niña and the negative AO years, and lower flows during El Niño and the positive AO years throughout most of the province (Figure 7, Tables A2 and A4). The phase relationship reversed in the very far north, where discharges were higher during the positive PDO, positive PNA, El Niño and positive AO years, rather than during the negative phase years. Patterns of streamflow variation according to climate oscillation phases closely followed the patterns of precipitation variation according to climate oscillation phases (Figures 2-5).

To the best of our knowledge, this study is the first to demonstrate these relationships between the four climate oscillations and Saskatchewan streamflow broadly across the province. *Burn et al*. (2008) undertook a similar study on small prairie streams and found no such relationships. Their study included only a quarter of the streamflow gauges examined in this study, was based upon shorter streamflow and climate oscillation records, used a lower threshold of climate oscillation events and was based upon a regular *t*-test with its normality assumptions that are inappropriate for small streams (*Gobena and Gan*, 2006). Monte Carlo permutation *t*-tests provide a straightforward method to handle the non-normality of annual mean daily discharge (*Manly*, 1998). Using the non-parametric (and therefore low-power) Mann-Whitney test, *Gobena and Gan* (2006) found that river discharge is higher during La Niña and negative PNA years in their collection of prairie streamflow records concentrated in Alberta, but which included three gauge records from Saskatchewan.

Any analysis of Saskatchewan hydroclimatology must work within the following limitations of the provincial streamflow datasets available through the Water Survey of Canada and the Saskatchewan Watershed Authority. The Saskatchewan hydrological records are the shortest of all such records in the Prairie Provinces, with a mean period of record of 48 years. Furthermore, there are no moderately-sized naturally-flowing rivers in the southern half of province, where because of extensive agriculture, an accurate portrait of the hydroclimatology is highly desired for water management. From a hydroclimatological perspective, this is a serious limitation as moderately sized rivers reflect the impact of the atmosphere-ocean climate oscillations much more strongly than small, flashy streams do, as the later are more impacted by small-scale, local, stochastic processes. Moderately-sized rivers have large enough watersheds to average the patchily distributed precipitation events, small streams do not. Lastly, only one low-frequency phase of the climate oscillations is well represented in the Saskatchewan hydrological period of record. In 1946, a predominately cool or negative PDO phase began. In 1977, the PDO shifted back into a warm phase, and in 2008, the PDO probably shifted back into the negative phase. The mean record commencement year is 1966 (with the exception of four longer, often discontinuous, records beginning in the 1910s), towards the end of the negative PDO phase (Figure 6). This results in there being very few annual mean daily discharges from negative PDO years available for analysis, which lessens the probability of detecting significantly different streamflows in the different phases. This also means that there are relatively few annual mean daily discharges from La Niña and negative PNA years, as both La Niña and negative PNA events are more likely to occur during the negative phase of the PDO (Figure 6). Similarly, discharges from negative AO years are underrepresented post-1975, as the AO has had a positive bias during these most recent 35 years. On the other hand, discharges from positive PDO, El Niño, positive PNA, and positive AO years are well represented in the hydrological record. This justifies in part this study's use of one-sample permutation *t*-tests.

There is one possible solution to the difficulty of the shortness of Saskatchewan streamflow records. Headwater streamflow records from Alberta and Manitoba are often longer in length, with a reasonable number of at least one PDO cycle in length (~60 years), and hence with good representation of discharge during negative PDO, La Niña, negative PNA and negative AO years. If the same composite analysis were to be repeated on the Manitoba and Alberta streamflow records and if such an analysis confirms this study's results of the relationships between streamflow and the climate oscillations, then our analysis is on a sounder and stronger footing. Our laboratory is in the midst of this extension as part of PRAC's mandate to further our understanding of Canadian prairie hydroclimatology.

Typically, hydrologists assume that the probability of extreme high or low flows is independently and identically distributed from year to year (*Franks and Kuczera*, 2002; *Kiem et al*., 2003). The application of this assumption to the Saskatchewan River Basin must be critically examined in light of this study's result that there is a definite asymmetry in the effect of PDO phase on the probability of two years of successive least (or highest) quartile flows of Saskatchewan River tributaries. Our laboratory is currently analyzing Saskatchewan River headwater flood and low flow return intervals segregated according to climate oscillation phase; and preliminary results suggest significant differences. As well, given that the probability of two years of successive least quartile flow is higher in the positive phase of the PDO, the probability of more than two years of low flow must be considered and the estimated basin reservoir capacity of at most two years should be re-evaluated. This is especially true in the light of the multi-centennial tree-ring inferred South Saskatchewan River record which shows periods of multi-decadal low flows in the past millennium (*Axelson et al*., 2010).

How exactly the upstream North Pacific Ocean affects the atmosphere, and hence the precipitation, temperature and hydrology, of the Canadian Prairies, and how the various atmosphere-ocean climate oscillations are mechanistically generated and how they interact and affect each other are active areas of research. The mechanism by which the PDO, or the zonal dipole in North Pacific SSTs, affects the hydroclimatology of the downstream western North America is a shift in the position of the sub-polar jet, which brings winter storms and precipitation, as it crosses over the edge of the continent (*Gershunov and Barnett*, 1998; *Bonsal et al*., 2001; *Stahl et al*., 2006). Whether or not the PDO is independent of ENSO is uncertain, but an active area of research. Some researchers (*e.g*., *Newman et al.,* 2003; *Schneider and Cornuelle*, 2005; *Newman*, 2007) have argued that ENSO drives the PDO, *i.e*., that El Niño (La Niña) drives the positive (negative) phase of the PDO. On the other hand, other researchers (*e.g*., *Zhang et al*., 1996; *Yu et al*., 2007) have considered the PDO to be independent of ENSO, but that reinforcing interactions could occur between the two oscillations. *Gershunov and Barnett* (1998), *Yu et al*. (2007) and *Wise* (2010) found that there occurred an enhanced response of the Pacific-North American mode (*Wallace and Gutzler*, 1981) when the PDO and ENSO were in the same phase; that is, when the PDO was in a negative phase and a La Niña occurred, the Pacific Northwest and western interior experienced cooler and wetter conditions than normal in a negative PDO alone. A positive AO winter is consistent with a negative PDO winter, as a more positive AO suggests a weaker Aleutian Low which is more consistent with the negative phase of the PDO (*Gershunov and Barnett*, 1998).

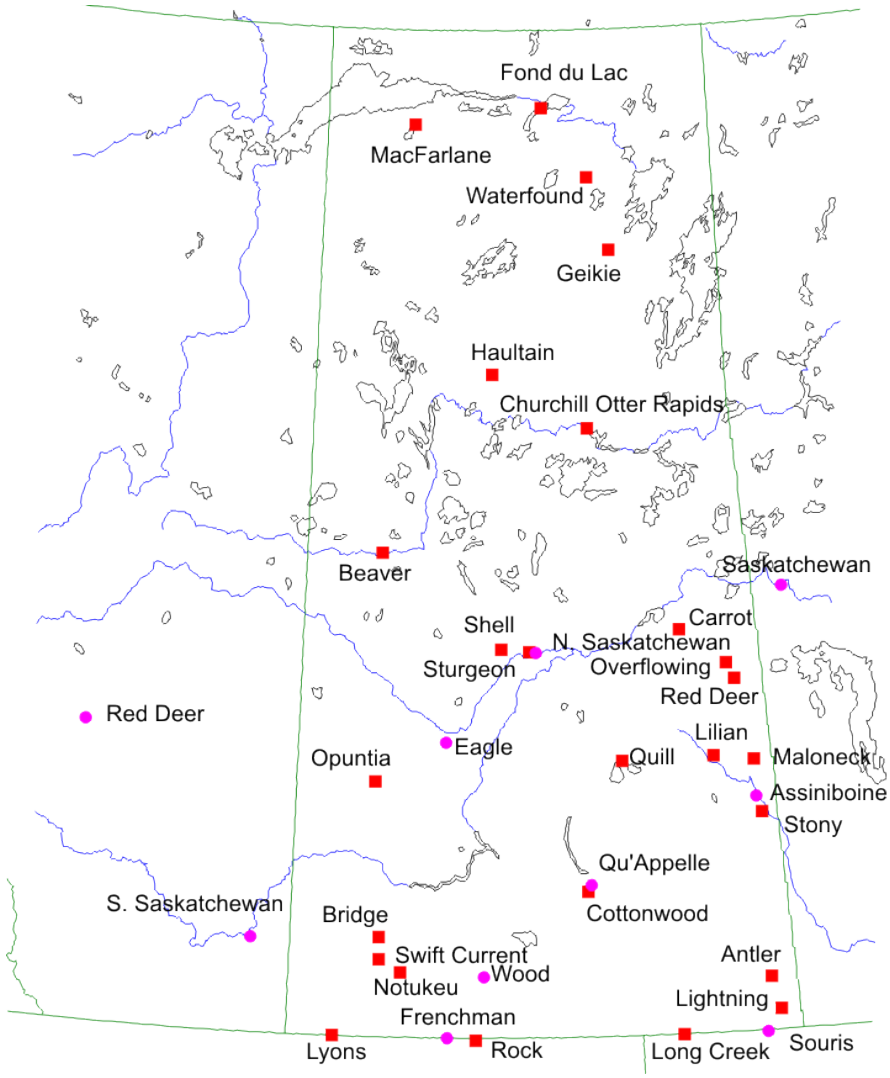

Figure 1. Twenty-six naturally-flowing river or stream flow records (red squares) and ten regulated flow river records (magenta circles) from Saskatchewan, Canada, and environs, used in this study.

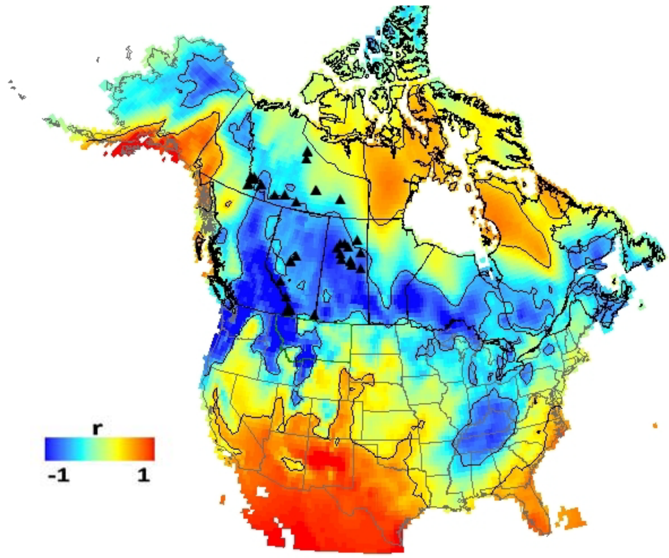

Figure 2. Correlations between same year winter (November-March) mean Pacific Decadal Oscillation (PDO) and concurrent North American precipitation for 1950-2000. ~10 km gridded climate data from the Canadian Forest Service Climate Dataset (*McKenney et al.*, 2006) (http://cfs.nrcan.gc.ca/subsite/glfc-climate/namonthly). Black line demarcates significance at the $p \leq 0.05$ level.

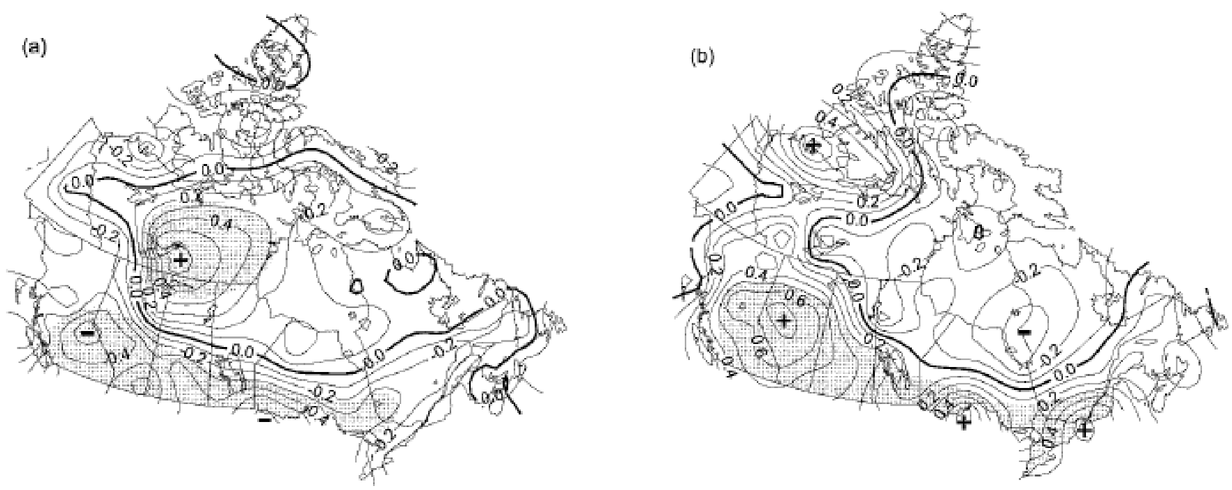

Figure 3. (a) Map of standardized precipitation anomalies for the January-March season following the onset of El Niño events [JFM(+1)], contour interval is 0.1. Shading denotes areas with precipitation anomalies significantly different from non-El Niño and non-La Niña periods using the Student's t-test and Wilcoxon rank-sum test (5% level). **(b)** Same as **(a)** but following the onset of La Niña events. Figure courtesy of *Shabbar et al.* (1997).

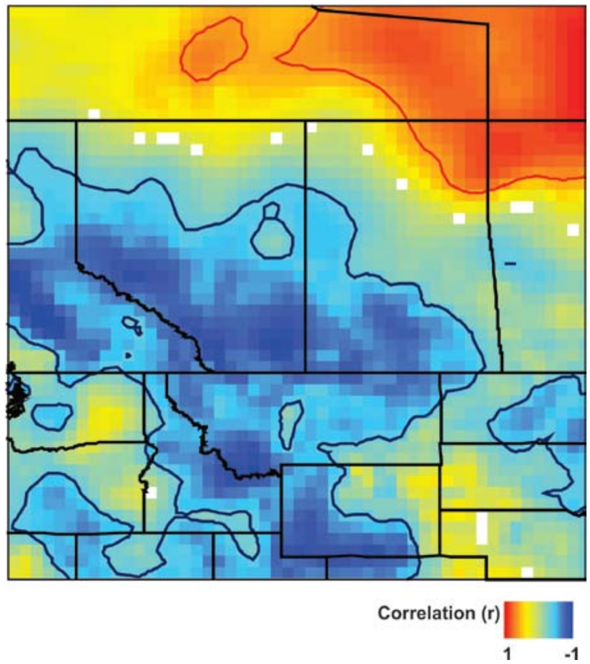

Figure 4. Correlations between same year winter (December-February) mean Pacific North American mode (PNA) and concurrent western interior precipitation for 1950-2000. ~10 km gridded climate data from the Canadian Forest Service Climate Dataset (*McKenney et al.,* 2006) (http://cfs.nrcan.gc.ca/subsite/glfc-climate/namonthly). Black line demarcates significance at the $p \leq 0.05$ level.

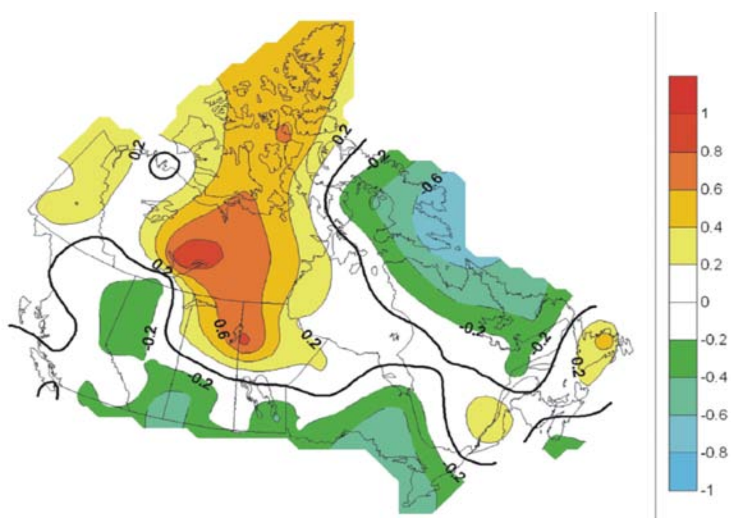

Figure 5. Correlation coefficients between winter (January to March) North Atlantic Oscillation (NAO), (as determined by the first rotated EOF of Northern Hemisphere mean sea level pressure) and concurrent precipitation over Canada for the period 1950 to 1999. Correlations greater than *0.36* in magnitude are significant at the *5%* level. NAO used as a proxy for the nearly identical Arctic Oscillation (AO). Figure courtesy of *Bonsal and Shabbar* (2008).

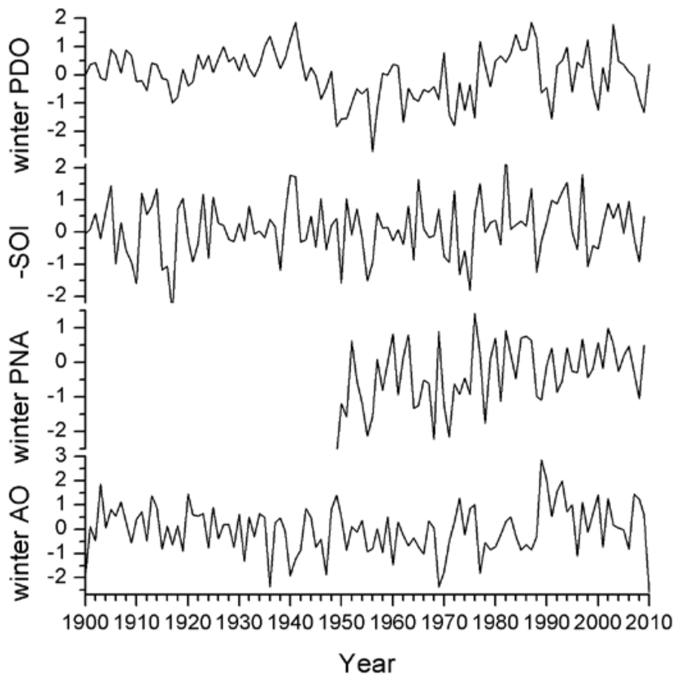

Figure 6. Plots of the November-March Pacific Decadal Oscillation (PDO), negative June-November Southern Oscillation Index (SOI), December-February Pacific North American mode (PNA) and December-March Arctic Oscillation (AO) for 1900-2010.

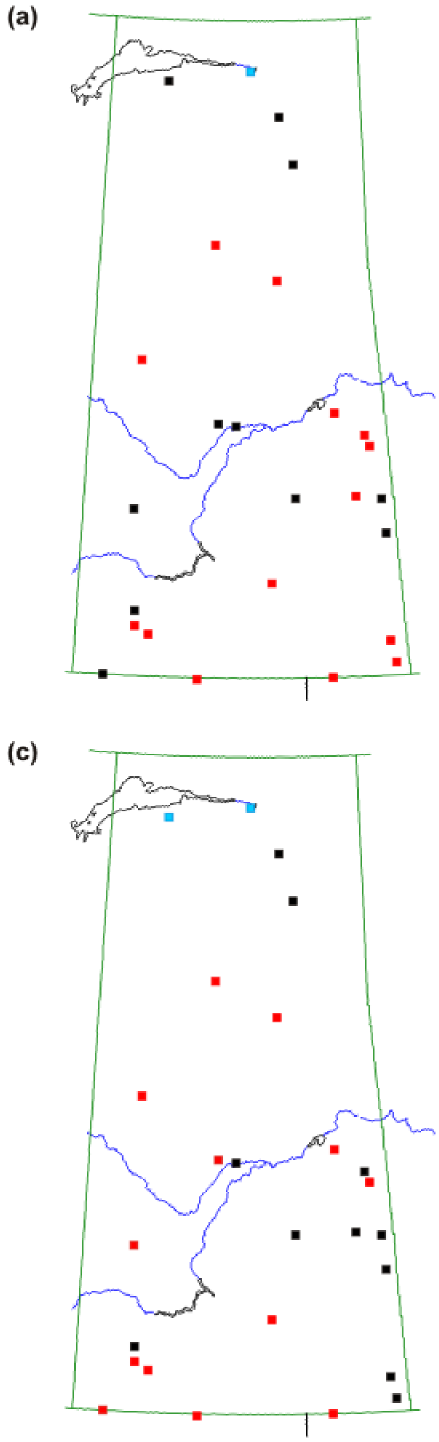

Figure 7. Fingerprints of the (a) Pacific Decadal Oscillation (PDO), (b) Southern Oscillation Index (SOI), (c) Pacific North American mode (PNA) and (d) Arctic Oscillation (AO) on Saskatchewan mean daily discharges. A red (blue) square denotes a significant negative (positive) relationship between the climate oscillation and mean daily discharge at the gauge location as assessed by a Monte Carlo permutation *t*-test at the *0.10* significance level. A black square denotes no significant relationship.

Table 1. Naturally-flowing river discharge records from Saskatchewan, including Water Survey of Canada gauge names, station codes, period of continuous or near-continuous record, number of years of record analyzed, effective drainage area, mean daily flow and location. Records ordered from south to north. If period of record is not equal to the number of years of record analyzed, it is because of missing years from unavailable gauge records.

Station name	WSC station code	Period of record	# yrs	Drainage area (km^2)	Mean daily flow (m^3/s)	Latitude (N)	Longitude (W)
Rock Creek below Horse Creek	11AE009	1916-1926, 1957-2009	64	830	0.77	48°58’10”	106°50’20”
Long Creek at West. Crossing*	05NA003	1912-2009	98	1,210	0.71	49°00’01”	103°21’08”
Lyons Creek at International Boundary	11AB075	1927-2009	83	136	0.09	49°00’17”	109°13’48”
Lightning Creek near Carnduff	05NF006	1974-2009	36	393	0.31	49°13’17”	101°43’08”
Antler River near Wauchope	05NF010	1965-2009	45	133	0.14	49°35’03”	101°50’52”
Notukeu Creek above Admiral Reservoir	05JB004	1975-2009	35	328	0.19	49°42’32”	108°07’31”
Swift Current Creek below Rock Creek	05HD036	1955-2009	55	1,090	1.30	49°50’40”	108°28’46”
Bridge Creek at Gull Lake	05HA015	1916-1922, 1963-2010	55	319	0.13	50°05’36”	108°29’38”
Cottonwood Creek near Lumsden	05JF011	1974-2009	36	224	0.34	50°35’26”	104°54’31”
Stony Creek near Kamsack	05MD010	1971-2009	39	116	0.31	51°23’19”	101°50’19”
Opuntia Lake West Inflow	05GC007	1960-2009	50	56.2	0.03	51°47’15”	108°37’30”
Maloneck Creek near Pelly	05LE011	1974-2010	37	171	0.50	51°58’08”	101°54’50”
Quill Creek near Quill Lake	05MA020	1973-2009	37	89.6	0.31	52°00’11”	104°14’50”
Lilian River near Lady Lake	05MC003	1970-2009	40	153	0.47	52°01’22”	102°37’30”
Red Deer River near Erwood	05LC001	1954-2009	56	8,550	22.9	52°51’36”	102°11’39”
Overflowing River near Hudson Bay	05LD003	1975-2010	36	349	1.84	53°01’51”	101°12’31”
Sturgeon River near Prince Albert	05GF002	1967-2008	42	2,560	3.14	53°12’47”	105°53’06”

Shell Brook near Shellbrook	05GF001	1966-2009	44	760	1.18	53^{o}15’10”	106^{o}23’09”
Carrot River near Smoky Burn	05KC001	1955-2008	54	7,120	16.0	53^{o}25’00”	103^{o}08’30”
Beaver River near Dorintosh	06AD001	1963-2009	47	16,900	29.17	54^{o}17’47”	108^{o}36’16”
Churchill River above Otter Rapids	06CD002	1964-2009	46	112,000	277.48	55^{o}38’47”	104^{o}44’05”
Haultain River above Norbert River	06BD001	1969, 1972-2009	39	3,680	18.46	56^{o}14’40”	106^{o}33’40”
Gelkie River below Wheeler River	06DA004	1967-2009	43	7,730	45.57	57^{o}35’20”	104^{o}12’10”
Waterfound River below Theriau Lake	07LB002	1975-1976, 1978-2009	34	3,160	21.31	58^{o}23’10”	104^{o}36’30”
MacFarlane River at Outlet of Davy Lake	07MB001	1968-2009	42	9,120	53.87	58^{o}58’00”	108^{o}10’30”
Fond du Lac River at Outlet of Black Lake**	07LE001, 07LE002	1947-2009	59	50,700	306.21	59^{o}8’50”	105^{o}32’20”

*Slightly regulated.

**Two nearby gauge records merged by drainage area ratio.

Table 2. Further information on the naturally-flowing river discharge records from Saskatchewan, including whether or not the gauge record is in the Reference Hydrometric Basin Network (RHBN) (*Harvey et al.*, 1999), season of flow available for analysis, coefficient of variation and normality assessment of analyzed discharge records. Normality was assessed using the Shapiro-Wilk *W* statistic, non-normal values at the *0.05* significance level in red bold font.

Station name	RHBN	Season analyzed	Coefficient of variation (%)	Shapiro-Wilk *W*	*p*-level
Rock Creek below Horse Creek	no	Mar.-Oct.	79.3	**0.9017**	**$9.25e^{-5}$**
Long Creek at Western Crossing	no	Jan.-Dec.	113.0	**0.7977**	**$2.80e^{-10}$**
Lyons Creek at International Boundary	yes	Mar.-Oct.	156.5	**0.6628**	**$1.65e^{-12}$**
Lightning Creek near Carnduff	yes	Mar.-Oct.	155.9	**0.6739**	**$1.13e^{-7}$**
Antler River near Wauchope	yes	Mar.-Oct.	167.5	**0.6070**	**$9.45e^{-10}$**
Notukeu Creek above Admiral Reservoir	yes	Mar.-Oct.	85.0	**0.9123**	**0.009**
Swift Current Creek below Rock Creek	no	Mar.-Oct.	55.9	**0.9190**	**0.001**
Bridge Creek at Gull Lake	no	Mar.-Oct.	118.8	**0.8100**	**$2.20e^{-6}$**

Cottonwood Creek near Lumsden	no	Mar.-Oct.	145.2	**0.7085**	**$3.86e^{-7}$**
Stony Creek near Kamsack	no	Mar.-Oct.	73.8	**0.8271**	**$3.20e^{-5}$**
Opuntia Lake West Inflow	no	Mar.-Oct.	116.3	**0.7769**	**$2.18e^{-7}$**
Maloneck Creek near Pelly	yes	Mar.-Oct.	76.2	**0.9014**	**0.003**
Quill Creek near Quill Lake	no	Mar.-Oct.	106.6	**0.8220**	**$3.73e^{-5}$**
Lilian River near Lady Lake	no	Mar.-Oct.	84.6	**0.8297**	**$3.00e^{-5}$**
Red Deer River near Erwood	no	Mar.-Oct.	83.7	**0.8184**	**$8.04e^{-7}$**
Overflowing River near Hudson Bay	yes	Mar.-Oct.	66.6	**0.8754**	**0.0008**
Sturgeon River near Prince Albert	no	Mar.-Oct.	82.1	**0.8512**	**$6.71e^{-5}$**
Shell Brook near Shellbrook	no	Mar.-Oct.	88.2	**0.7795**	**$1.08e^{-6}$**
Carrot River near Smoky Burn	no	Mar.-Oct.	82.1	**0.8862**	**$9.80e^{-5}$**
Beaver River near Dorintosh	no	Mar.-Oct.	75.8	**0.8417**	**$1.57e^{-5}$**
Churchill River above Otter Rapids	yes	Jan.-Dec.	38.8	0.9526	0.059
Haultain River above Norbert River	yes	Jan.-Dec.	27.0	0.9618	0.205
Gelkie River below Wheeler River	yes	Jan.-Dec.	22.4	**0.8959**	**0.001**
Waterfound River below Theriau Lake	no	Jan.-Dec.	14.7	0.9518	0.162
MacFarlane River at Outlet of Davy Lake	no	Jan.-Dec.	15.9	0.9666	0.253
Fond du Lac River at Outlet of Black Lake*	yes*	Jan.-Dec.	16.9	0.9808	0.476

*07LE002 in the RHBN, 07LE001 not in the RHBN, has been discontinued.

Table 3. Classification of years into strong positive and negative climate oscillation events for the Pacific Decadal Oscillation (PDO), Southern Oscillation Index (SOI), Pacific North American mode (PNA) and Arctic Oscillation (AO) (see text for full definitions).

Climate Oscillation	**Phase**	**Strong event years**
PDO	**positive**	1905, 1906, 1908, 1909, 1922, 1924, 1927, 1931, 1935, 1936, 1937, 1940, 1941, 1942, 1970, 1977, 1981, 1983-1988, 1994, 1998, 2003
	negative	1917, 1918, 1946, 1949, 1950, 1951, 1952, 1954, 1956, 1957, 1962, 1964, 1965, 1969, 1971, 1972, 1974, 1976, 1991, 2000, 2008, 2009
SOI	**positive La Niña**	1906, 1908, 1909, 1910, 1915, 1916, 1917, 1921, 1924, 1938, 1945, 1947, 1950, 1955, 1956, 1964, 1970, 1971, 1973, 1974, 1975, 1988, 1996, 1998, 2000, 2008
	negative El Niño	1902, 1904, 1905, 1911, 1912, 1913, 1914, 1918, 1919, 1923, 1925, 1932, 1939, 1940, 1941, 1944, 1946, 1951, 1953, 1957, 1963, 1965, 1969, 1972, 1976, 1977, 1982, 1987, 1991, 1992, 1993, 1994, 1997, 2002,

		2004, 2006, 2009
PNA	**positive**	1953, 1961, 1964, 1970, 1977, 1981, 1983, 1986, 1987, 1988, 1992, 1995, 1998, 2001, 2003, 2004, 2007, 2010
	negative	1950, 1951, 1952, 1955, 1956, 1957, 1965, 1966, 1969, 1971, 1972, 1979, 1982, 1990, 2009
AO	**positive**	1903,1905, 1907, 1913, 1914, 1920, 1925, 1943, 1948, 1949, 1973, 1975, 1976, 1989, 1990, 1992, 1993, 1995, 1997, 2000, 2002, 2007, 2008
	negative	1900, 1915, 1919, 1931, 1936, 1940, 1941, 1942, 1947, 1951, 1955, 1956, 1958, 1960, 1966, 1969, 1970, 1977, 1979, 1985, 1987, 1996, 2006, 2010

Table 4. Empirical probabilities of two successive years of least quartile and highest quartile flows composited according to Pacific Decadal Oscillation (PDO) phase for the Saskatchewan River and its tributaries in Alberta, Saskatchewan and Manitoba.

Streamflow record	Prob. 2 successive yrs least 1/4 flow in +PDO phase	Prob. 2 successive yrs least 1/4 flow in –PDO phase	Prob. 2 successive yrs highest 1/4 flow in +PDO phase	Prob. 2 successive yrs highest 1/4 flow in –PDO phase
Marias R. near Shelby, MT [06099500]	0.157	0.000	0.020	0.146
Waterton R. near Waterton Park [05AD003]	0.118	0.000	0.039	0.122
Castle R. near Beaver Mines [05AA022]	0.097	0.034	0.000	0.138
Oldman R. near Waldron's Corner[05AA023]	0.167	0.000	0.033	0.077
Highwood R. at Diebel's Ranch [05BL019]	0.194	0.000	0.033	0.042
Bow R. at Banff [05BB001]	0.115	0.000	0.078	0.071
Columbia R. at Nicholson, BC [08NA002]	0.118	0.000	0.059	0.056
Red Deer R. at Red Deer [05CC002]	0.098	0.122	0.039	0.171
Naturalized St. Mary R. at Int. Boundary	0.133	0.000	0.044	0.098
Actual St. Mary R. at Int. Boundary [05AE027]	0.157	0.020	0.020	0.160
Naturalized Belly R. near Mountain View	0.111	0.000	0.022	0.146
Actual Belly R. near Mountain View [05AD005]	0.098	0.000	0.039	0.122
Naturalized Oldman R. near Lethbridge	0.200	0.000	0.067	0.146

Actual Oldman R. near Lethbridge [05AD007]	0.196	0.000	0.020	0.146
Naturalized S. Saskatchewan R. at Medicine Hat	0.200	0.000	0.022	0.171
Actual S. Saskatchewan R. at Medicine Hat [05AJ001]	0.196	0.000	0.020	0.171
Naturalized Elbow R. below Glenmore Dam	0.200	0.000	0.044	0.146
Actual Elbow R. below Glenmore Dam [05BJ001]	0.176	0.048	0.059	0.190
Naturalized Bow R. at Calgary	0.178	0.000	0.044	0.195
Actual Bow R. at Calgary [05BH004]	0.176	0.024	0.039	0.195
Naturalized Spray R. at Banff	0.133	0.000	0.067	0.122
Naturalized N. Saskatchewan R. at Edmonton	0.118	0.024	0.098	0.119
Actual N. Saskatchewan R. at Edmonton [05DF001]	0.118	0.024	0.078	0.122
Actual N. Saskatchewan R. at Prince Albert, SK [05GG001]	0.137	0.049	0.039	0.122
Actual Saskatchewan R. at the Pas, MB [05KJ001]	0.137	0.025	0.059	0.175
Mean	0.149	0.015	0.043	0.135

Part II. Trends in Saskatchewan Stream and River Discharges

Introduction and methods

In this section we examine Saskatchewan river annual mean daily flow records for trends. There are many problems with analyzing the instrumental streamflow records simplistically using methods such as ordinary least squares regression techniques. These records can be discontinuous, and are short, typically having periods of record of ~35-50 years in Saskatchewan with a few exceptions. The naturally-flowing rivers in the south are basically streams which can have years of no flow, but also outlier years of exceptionally high flows, i.e, extremely flashy flows with an very non-normal distribution (Table 2). There is frequent positive autocorrelation in many river discharge time series, which results in the overestimation of the effective sample size of the residuals in classical linear regression and Mann-Kendall non-parametric methods (*Zheng et al.* 1997). Therefore, these methods will disproportionately reject a null hypothesis of no trend (*Zheng et al.*, 1997; *Zhang et al.*, 2001; *Burn and Hag Elnur*, 2002; *Yue et al.*, 2002a). Lastly, there is heavy human impact from water consumption, diversion and storage, especially in the larger rivers of southern Saskatchewan, which overlays and obscures the natural hydrology.

Trends in annual mean daily flow (m^3/s) over the entire period of record were assessed by the non-parametric Mann-Kendall (MK) statistical test (*Mann*, 1945; *Kendall*, 1975). The MK test is widely used to assess the significance of trend in hydrological time series (*Burn*, 1994; *Helsel and Hirsch*, 2002; *Khaliq et al.*, 2009). The MK test searches for a trend in a time series without specifying whether the trend is linear or nonlinear. It is based on the test statistic *S*, where

$$S = \sum_{i=1}^{N-1} \sum_{j=i+1}^{N} signum\ (Y_j - Y_i)$$

where Y_i and Y_j are the sequential flow data, *N* is the length of the time series and

$$signum\ (Y_j - Y_i) = 1\ if\ (Y_j - Y_i) > 0;$$

$$signum\ (Y_j - Y_i) = 0\ if\ (Y_j - Y_i) = 0;$$

$$signum\ (Y_j - Y_i) = -1\ if\ (Y_j - Y_i) < 0.$$

A positive (negative) value of *S* demonstrates an increasing (decreasing) trend. For $N \geq 10$, *Mann* (1945) and *Kendall* (1975) have proven that *S* is approximately normally distributed with the mean $E(S) = 0$ and

$$Var\ (S) = \frac{[N(N-1)(2N+5) - \sum_{i=1}^{n} t_i i(i-1)(2i+5)]}{18}$$

where t_i is the number of ties of extent *i* (*i.e.*, the size of the tied group) and *n* is the number of tied groups. The standardized test statistic *Z* based upon *S* follows the standard normal distribution.

$$Z = \begin{cases} \dfrac{(S-1)}{\sqrt{Var(S)}} & if\ S > 0 \\ 0 & if\ S = 0 \\ \dfrac{(S+1)}{\sqrt{Var(S)}} & if\ S < 0 \end{cases}$$

At significance level α, the null hypothesis of no trend is rejected if the absolute value of *Z* is greater than the theoretical value $Z_{(1-\alpha)/2}$.

However, the MK test needs data to be serially independent, a condition often not met with hydrological data. To remove the effect of serial correlation on the MK test, we use a variance correction approach (VC) (also called an effective sample size (ESS) approach) (*Yue and Wang*, 2004). As described by *Bayley and Hammersley* (1946), the VC approach rests upon the fact that *N* serially correlated observations contain the same information as $N^* < N$ uncorrelated observations. The presence of autocorrelation in a time series changes *Var(S),* although it does not change *mean(S)* or alter the asymptotic normality of the MK test statistic *S* (*Hamed and Rao*, 1998; *Yue et al*., 2002a; *Yue and Wang*, 2004). *Yue and Wang* (2004) suggest correcting *Var(S)* by using an effective sample size that reflects the degree of autocorrelation present, *i.e., Var*(S)* = correction factor *CF* * *Var(S)* where $CF = 1 + 2\sum_{k=1}^{N-1}(1-\frac{k}{N})r_k$ and r_k is the lag-*k* serial correlation coefficient of the data. In practice, an AR(1) process is reasonable for much annual mean daily flow data; therefore, we only use r_1, so

$$CF = 1 + 2 \cdot \frac{r_1^{N+1} - N \cdot r_1^2 + (N-1) \cdot r_1}{N\,(r_1 - 1)^2}$$

where if $X_1, X_2, \ldots, X_N$ is the hydrological time series, then

$$r_1 = \frac{\frac{1}{N-1}\sum_{t=1}^{N-1}(X_t - \bar{X}_t)(X_{t+1} - \bar{X}_t)}{\frac{1}{N}\sum_{t=1}^{N}(X_t - \bar{X}_t)^2}$$

and

$$\bar{X}_t = \frac{1}{N}\sum_{t=1}^{N} X_t$$

(*Yue and Wang*, 2004; *Khaliq et al.*, 2009). *Yue and Wang* (2004) showed that the existence of trend in a time series contaminates the estimate of the true serial correlation; and therefore, if the contaminated serial correlation is used to derive *CF*, then the effect of the true serial correlation on the MK test cannot be properly eliminated. Hence, the trend component is removed first, leaving the detrended residual series of an AR(1) process and noise (*Yue and Wang*, 2004). The sample lag-one autocorrelation coefficient, r_1, is then computed from this detrended residual series. If a record was discontinuous, r_1 was calculated from the longest continuous segment. Lastly, the modified MK test with VC is then applied to the original time series to access the trend significance. The trend is removed using a robust, rank-based, non-parametric Sen-Theil line, where β_1 is the estimate of the trend slope and β_0 is the estimate of the intercept (*Theil*, 1950; *Sen*, 1968).

$$\beta_1 = median\left(\frac{(X_j - X_l)}{j - l}\right) \forall\, l < j$$

$$\beta_0 = median(1,2, \dots, N) - \beta_1 \cdot median\,(X_1, X_2, \dots, X_N)$$

Significance levels of $p \leq 0.05$ and $0.05 \leq p \leq 0.1$ were used in trend detection following standard hydrological practice (*Smith et al.*, 2007). *Khaliq et al.* (2009) in their evaluation of hydrological trend detection methods considered the modified MK test with variance correction and an AR(1) assumption to be one of the best performing analysis methods.

Both the 26 relatively unregulated flow records in Part I of this report (Table 1) and 10 important regulated flow records from Saskatchewan and environs are examined (Tables 5 and 6). If only warm season flow data were available, we examined mean daily flow data averaged over March-October. Otherwise, if twelve months of data were available, we examined data annualized over the calendar year (January-December). All available data were analyzed, even if discontinuous. If a gauge had a large segment of data from the 1910s and 1920s, then a hiatus, and then data beginning again in the 1950s or 1960s, the time series was analyzed both with and without the initial segment. The magnitude of the changes in estimated mean daily flow over the period of individual record were calculated by the Sen-Theil line and reported as both total percentage changes from the beginning of record, and *per annum*.

Results

The modified Mann-Kendall test showed three significant trends at the *0.05* significance level and one at the *0.1* significance level in the 26 naturally-flowing daily mean time series (Table 7 and Figure 8). There were four significant declining trends and no significant increasing trends. The four significant declining trends at Rock Creek, Lyons Creek, Bridge Creek and Beaver River gauges were clustered in the southwest corner of the province. Rock Creek, Lyons Creek and Beaver River were significant at the *0.05* significance level. Rock Creek and Bridge Creek have discontinuous records that began in 1910s and ended in the 1920s and then started again circa 1960. Rock Creek showed a significant decline in the shorter continuous time segment of 1957-2009. However, Bridge Creek showed a non-significant decline in the shorter continuous time segment of 1963-2010, so including the earlier data affects analysis.

The modified Mann-Kendall test showed four significant trends at the *0.05* significance level in the 10 regulated-flow daily mean time series (Table 7 and Figure 8). There were three significant declining trends located at the Frenchman River, the South Saskatchewan River at Medicine Hat and the Saskatchewan River at Le Pas gauges and one significant increasing trend at the Qu'Appelle River gauge. The Qu'Appelle River has a discontinuous record with sparse data in 1910s, 1920s and early 1940s, and then a continuous record for 1947-2009. The Qu'Appelle record showed a significant increase in both the entire record and in the shorter continuous time segment of 1947-2009.

Discussion

There is a decline in annual mean daily flow in the naturally-flowing streams in the southwest corner of the province (Figure 8). With a 5% significance level, one would expect ~1.3 = 5% of the 26 naturally-flowing streams to show a significant trend by chance; and there to be no geographical pattern in the chance trends, nor consistency of trend sign. The geographical cluster of three declining streams in the southwest suggests that this pattern has not occurred due to chance, even if it is only three of the five regional streams. *Zhang et al.* (2001), using the MK test on prewhitened data, found similar results of declining annual mean streamflow in the southwest corner of Saskatchewan over a different period of record. The three declining gauge records in the southwest corner are among the longest streamflow records in Saskatchewan, beginning in the 1910s; therefore, the declines are not just artifacts of the PDO phase. The ~60 year low frequency cycle of the PDO can potentially generate a declining linear trend in short instrumental streamflow records. Many western North American instrumental streamflow records begin in the 1950s or 1960s (a period of strongly negative PDO, hence high prairie streamflow), or omit the 1930s and 1940s (periods of high positive PDO, hence low prairie streamflow). Therefore, any trend line fit between this initial high flow period, followed by this subsequent low flow period shows a declining trend. If the influence of the PDO is not taken into account in an analysis of prairie instrumental hydroclimatic records, this could produce detected declines that could be attributed to climate change, while they are actually artifacts of the sampling period and the PDO phase changes (*e.g., Chen and Grasby*, 2009). Very few streamflow trend analyses consider the issue of PDO phase. The non-parametric Mann-Kendall test used in the analysis is a relatively low-powered test, *i.e.*, a serious decline must have taken place before the MK test is able to detect it (*Sokal and Rohlf*, 1995; *Yue et al.*, 2002b). There could be significant declines present that a more powerful test could detect. The climatology of this southwest corner is closely coupled to the southernmost portion of the Alberta prairies, which is also showing declining trends in its naturally-flowing stream gauge records (*Rood et al.* 2005, 2008; *St. Jacques et al.*, 2010).

There also are significant declines in the regulated flows of the South Saskatchewan River Basin (Figure 8). This is in accord with previous Alberta-focused studies (*i.e., Rood et al.*, 2005; 2008; *Schindler and Donahue,* 2006; *St. Jacques et al.,* 2010). *St. Jacques et al.* (2010) showed that the basin declines were due to both direct human impact and climatic changes, with both effects being approximately equal in magnitude. The worst of the decline is in the southern Oldman and Bow River Basins, as the downstream gauge at Medicine Hat shows a very significant decline, and not in the northern Red Deer River Basin, which shows a non-significant decline. This decline propagates all the way downstream to the gauge at Le Pas, which shows a highly significant decline. The decline in the Frenchman River flow must be evaluated in the context of this drying of the southwest corner, as it is likely due to both climate change and human impact. In southern Alberta, there is a bad pattern of a drying climate (which results in less river discharge) triggering more water use for irrigation, which results in further reductions of discharge. The increase in Qu'Appelle River flow is most likely due to diversions from Lake Diefenbacher, as the nearby naturally-flowing Cottonwood Creek shows no increase.

Apart from the southwest corner (and western, central Beaver River), annual naturally-flowing hydrological series through-out the rest of the province show no significant trends when tested over their entire period of record. In their MK-based analysis of Adjusted Historical Canadian Climate Data, *Zhang et al*. (2000) showed that Saskatchewan has become significantly warmer over the past century, as well as wetter (significantly wetter in the north). Hence, our streamflow analysis suggests that either increased evaporation from higher temperatures is balanced by increased precipitation throughout much of the province, or that emerging trends in the very short hydrological time series are still below the threshold of detection of the weak MK test. Mention detected seasonal shifts here. Compare to Burn's results and Zhang, Gan. Immediately to the north of Saskatchewan, rivers in the Northwest Territories are showing increases in annual discharge and winter baseflow due to hydrological cycle intensification and melting permafrost from anthropogenic global warming (*St. Jacques and Sauchyn*, 2009). This study detects no increased flow in the Saskatchewan far north where sporadic permafrost is present.

An assessment of any MK trend analysis must be placed in the context of recent advances in hydrological statistics. It has only relatively recently been widely appreciated that the MK test is affected by the serial correlation present in many hydrological time series (*Kulkarni and von Storch*, 1995). If there is positive (negative) autocorrelation in a time series, the MK test will suggest a significant trend in the series (which is actually random) more (less) often than specified by the significance level. *Gan* (1998) did not directly address the issue of autocorrelation, but rather analyzed monthly mean flows, assuming autocorrelation was negligible (an assumption that seems to need testing). There are various methods of dealing with this problem: at the very least, testing to see if autocorrelation is actually present or not (*e.g*., *St. Jacques and Sauchyn*, 2009), a variance correction or effective sample size correction to the test, such as that used in this study (*Yue and Wang*, 2004), or pre-whitening, that is, removal of the autocorrelation before testing (*Kulkarni and von Storch*, 1995; *Zhang et al*., 2000, 2001; *Yue et al*., 2002). There are different, often controversial, approaches to prewhitening. One is to estimate the lag-one autocorrelation coefficient r_1 directly from the time series, and then prewhitening the time series ($y_i = x_i - r_1 x_{i-1}, \forall\, i$) (*Kulkarni and von Storch*, 1995; *Zhang et al*., 2001). This was the approach used by *Zhang et al.* (2001). The problem with this approach is that if a trend is present in the time series, together with positive autocorrelation; it biases the estimation of r_1, affects the magnitude of estimated slope and leads to an increased chance of accepting the null hypothesis of no trend when a trend is actually present (*Yue et al*., 2002; *Khaliq et al*., 2009). As a correction,*Yue et al.* (2002) proposed another prewhitening method: for a given time series, detrend it by a Sen-Theil line, estimate the lag-one autocorrelation coefficient r_1 in the detrended time series, prewhiten the detrended time series using r_1, add back in the trend, and then apply the MK test to the final time series. This is the approach followed by *Burn et al.* (2008). Unfortunately, this complex method leads to an over-rejection of the no trend null hypothesis (*Khaliq et al*., 2009). Lastly, there is an iterative method based on successive estimation of r_1 and β (the slope coefficient) which seems reasonable, but whose performance is unknown. This is the method used by *Zhang et al*. (2000). In their recent assessment of the different Mann-Kendall methods, *Khaliq et al*. (2009) concluded that the use of a variance correction method such as that used here or a bootstrapping approach (*e.g., Kundzewicz and Robson*, 2000) is best practice.

Conclusions

This study detects the fingerprints of the PDO and the PNA on annual discharge in Saskatchewan streams and rivers, with increased flows during the negative phases of the PDO and the PNA, and decreases flows during the positive phases. A lesser fingerprint of ENSO and the AO are also detected. Because of the ~60-year cycle of the PDO, this has important implications in the detection of emerging trends in streamflow in response to global climate change. Separation of emerging trend from PDO phase artifact is greatly facilitated in streamflow time series that span at least one PDO cycle, preferably one and a half cycles, especially in the small prairie streams where parametric statistical methods are inappropriate. This highlights the continued importance of the stream gauge monitoring programs maintained by the Saskatchewan Watershed Authority and the Water Survey of Canada. A modified MK trend analysis of Saskatchewan streams shows decreasing flows in the southwest and in the Saskatchewan River and its southern tributaries.

Dave need your magic here.

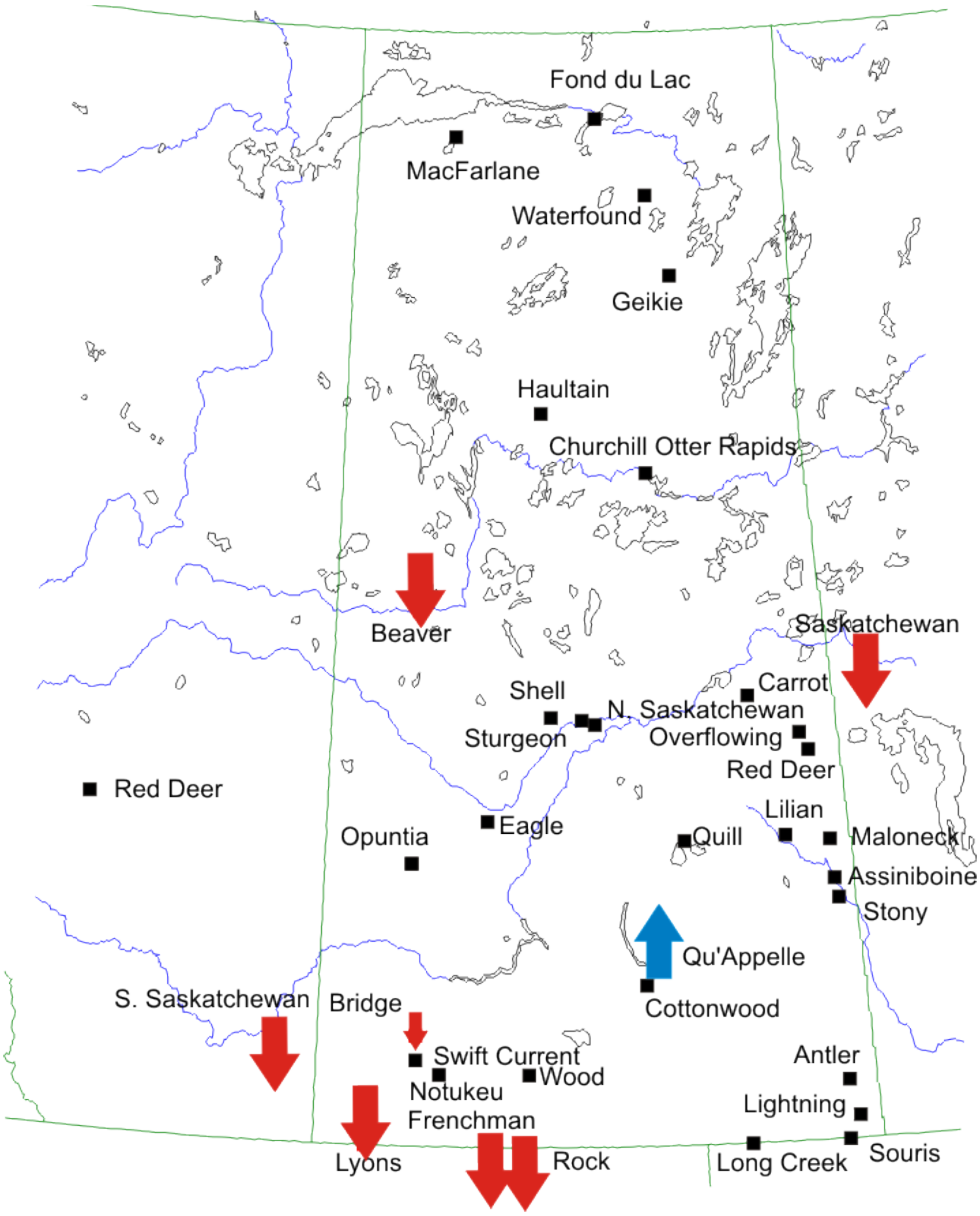

Figure 8. Geographic pattern of trends in annual mean daily streamflow from Saskatchewan and environs. A large red down (blue up) arrow denotes a decreasing (increasing) trend at the *0.05* significance level, a small red down (blue up) arrow denotes a decreasing (increasing) trend at the *0.1* significance level. A black square denotes no significant trend at the gauge at that location.

Table 5. Regulated-flow river discharge records from Saskatchewan and environs, including Water Survey of Canada gauge names, station codes, period of continuous or near-continuous record, number of years of record analyzed, effective drainage area, annual mean daily flow and location. Records ordered from south to north. If period of record is not equal to the number of years of record analyzed, it is because of missing years from unavailable gauge records.

Station name	WSC [USGS] station code	Period of record	# yrs	Drainage area (km^2)	Mean daily flow (m^3/s)	Latitude (N)	Longitude (W)
Souris River near Sherwood, N.D.	05114000	1931-2009	79	7,874	3.4	48°59’24”	101°57’28”
Frenchman River at the International Boundary	11AC041	1917-2009	93	4,630	3.0	49°00’00”	107°18’08”
Wood River near LaFleche	05JA002	1957-2009	53	3,760	2.0	49°40’01”	106°41’33”
S. Saskatchewan River at Medicine Hat	05AJ001	1912-2009	98	41,376	186.5	50°02’32”	110°40’39”
Qu’Appelle River near Lumsden	05JF001	1912-22, 1929-30, 1944-45, 1947-2009	78	6,950	6.9	50°39’16”	104°51’06”
Assiniboine River at Kamsack	05MD004	1950-2009	60	4,320	10.2	51°33’53”	101°54’58”
Eagle Creek near Environ	05GC006	1963-2009	47	2,090	1.2	52°13’50”	107°22’40”
Red Deer River at Red Deer	05CC002	1912-2009	98	11,052	47.6	52°16’35”	113°49’02”
N. Saskatchewan River at Prince Albert	05GG001	1912-2009	98	72,300	238.3	53°12’12”	105°46’19”
Saskatchewan River at Le Pas	05KJ001	1913-2009	97	389,000	621.9	53°50’17”	101°12’31”

Table 6. Further information on the regulated-flow river discharge records from Saskatchewan, including whether or not the gauge record is in the Reference Hydrometric Basin Network (RHBN) (*Harvey et al.*, 1999), season of flow available for analysis, coefficient of variation and normality assessment of analyzed discharge records. Normality was assessed using the Shapiro-Wilk *W* statistic, non-normal values at the *0.05* significance level in red bold font.

Station name	RHBN	Season analyzed	Coefficient of variation (%)	Shapiro-Wilk *W*	*p*-level
Souris River near Sherwood, N.D.	no	Jan.-Dec.	126.0	**0.7326**	**$1.09e^{-10}$**
Frenchman River at the International Boundary	no	Mar.-Oct.	98.0	**0.7445**	**$2.01e^{-11}$**

Wood River near LaFleche	no	Mar.-Oct.	105.8	**0.8387**	**$4.61e^{-7}$**
S. Saskatchewan River at Medicine Hat	no	Jan.-Dec.	38.6	**0.9680**	**0.017**
Qu'Appelle River near Lumsden	no	Mar.-Oct.	86.7	**0.8577**	**$3.87e^{-7}$**
Assiniboine River at Kamsack	no	Mar.-Oct.	92.8	**0.8391**	**$1.47e^{-6}$**
Eagle Creek near Environ	no	Mar.-Oct.	109.0	**0.7957**	**$1.27e^{-6}$**
Red Deer River at Red Deer	no	Jan.-Dec.	42.3	**0.8941**	**$9.32e^{-7}$**
N. Saskatchewan River at Prince Albert	no	Jan.-Dec.	24.7	**0.9447**	**0.0004**
Saskatchewan River at Le Pas	no	Jan.-Dec.	29.6	**0.9578**	**0.003**

Table 7. Modified Mann-Kendall (MK) trend tests on Saskatchewan mean daily river records. All available data were analyzed, even if discontinuous. The coefficients from the Sen-Theil lines are $\widehat{\beta_0}$ (the intercept) and $\widehat{\beta_1}$ (the slope); S is the Mann-Kendall score; $Var^*(S)$ is the modified variance; r_1 is the sample lag-one autocorrelation coefficient from the detrended time series; Z is the modified Mann-Kendall z-score; p-level is the result of the two-tailed modified MK test on $|Z|$ at the *0.1* significance level (bold red or blue denotes a significant trend).

Station name	$\widehat{\beta_0}$	$\widehat{\beta_1}$	S	$Var^*(S)$	r_1	CF	Z	p-level	Significant trend
Naturally flowing streams									
Rock Creek below Horse Creek	13.56	-0.007	-464	26,891	-0.052	0.903	-2.823	**0.005**	**decreasing**
Long Creek at West. Crossing	0.841	-0.0002	-50	128,697	0.097	1.212	-0.137	0.891	none
Lyons Creek at International Boundary	0.956	-0.0004	-660	58,117	-0.044	0.917	-2.734	**0.006**	**decreasing**
Lightning Creek near Carnduff	0.465	-0.0002	-35	8,704	0.242	1.615	-0.364	0.716	none
Antler River near Wauchope	1.927	-0.001	-182	18,916	0.295	1.811	-1.316	0.188	none
Notukeu Creek above Admiral Reservoir	-3.392	0.002	69	3,581	-0.166	0.722	1.136	0.256	none
Swift Current Creek below Rock Creek	14.630	-0.007	-157	16,243	-0.079	0.856	-1.224	0.221	none
Bridge Creek at Gull Lake	1.263	-0.0006	-215	16,204	-0.080	0.854	-1.681	**0.093**	**decreasing**
Cottonwood Creek near Lumsden	3.685	-0.002	-70	7,161	0.146	1.331	-0.815	0.415	none
Stony Creek near Kamsack	-4.966	0.003	91	5,214	-0.138	0.763	1.246	0.213	none
Opuntia Lake West Inflow	0.503	-0.0002	-173	25,000	0.250	1.649	-1.088	0.277	none
Maloneck Creek near Pelly	-9.540	0.005	64	10,665	0.301	1.828	0.610	0.542	none
Quill Creek near Quill Lake	-5.182	0.003	60	11,058	0.317	1.892	0.561	0.575	none
Lilian River near Lady Lake	6.324	-0.003	-66	11,436	0.222	1.552	-0.608	0.543	none

Red Deer River near Erwood	274.5	-0.129	-152	53,793	0.466	2.687	-0.651	0.515	none
Overflowing River near Hudson Bay	-59.665	0.031	127	6,756	0.116	1.254	1.533	0.125	none
Sturgeon River near Prince Albert	0.487	0.001	5	22,326	0.459	2.622	0.027	0.979	none
Shell Brook near Shellbrook	-1.523	0.001	18	20,984	0.373	2.147	0.117	0.907	none
Carrot River near Smoky Burn	266.2	-0.129	-189	43,157	0.420	2.402	-0.905	0.365	none
Beaver River near Dorintosh	1,026.3	-0.506	-301	22,931	0.324	1.928	-1.981	**0.048**	**decreasing**
Churchill River above Otter Rapids	2,181.9	-0.968	-72	44,640	0.614	4.002	-0.336	0.737	none
Haultain River above Norbert River	-122.3	0.071	69	14,456	0.368	2.117	0.566	0.572	none
Gelkie River below Wheeler River	143.1	-0.05	-42	9,125	0.552	3.336	-0.235	0.814	none
Waterfound River below Theriau Lake	84.348	-0.032	-26	6,511	0.183	1.432	-0.310	0.757	none
MacFarlane River at Outlet of Davy Lake	-57.17	0.056	41	8,510	0.448	2.553	0.271	0.786	none
Fond du Lac River at Outlet of Black L.	-711.6	0.512	200	77,934	0.548	3.334	0.779	0.476	none
Regulated-flow streams									
Souris River near Sherwood, N.D.	-1.277	0.001	53	89,883	0.237	1.611	0.173	0.862	none
Frenchman River at the Int. Bound.	52.84	-0.026	-1,088	111,166	0.102	1.224	-3.260	**0.001**	**decreasing**
Wood River near LaFleche	25.89	-0.012	-166	14,607	-0.077	0.860	-1.365	0.172	none
S. Saskatchewan River at Medicine Hat	1,773.8	-0.814	-1,071	171,533	0.238	1.616	-2.584	**0.010**	**decreasing**
Qu'Appelle River near Lumsden	-122.9	0.065	895	78,684	0.191	1.465	3.187	**0.001**	**increasing**
Assiniboine River at Kamsack	-27.55	0.018	54	64,060	0.453	2.606	0.209	0.834	none
Eagle Creek near Environ	16.37	-0.008	-141	20,260	0.266	1.704	-0.984	0.325	none
Red Deer River at Red Deer	181.3	-0.071	-359	215,257	0.343	2.028	-0.772	0.440	none
N. Saskatchewan River at Prince Albert	853.9	-0.32	-485	106,129	0.169	1.402	-1.255	0.210	none
Saskatchewan River at Le Pas	4,730	-2.115	-1007	237,840	0.400	2.310	-2.063	**0.039**	**decreasing**

References

Axelson, J., D. J. Sauchyn and J. Barichivich (2010), New reconstructions of streamflow variability in the South Saskatchewan River basin from a network of tree-ring chronologies, Alberta, Canada, *Water Resour. Res.*

Bayley GV, Hammersley JM. 1946. The effective number of independent observations in an autocorrelated time series. *Journal of the Royal Statistical Society* **8**: 184-197.

Bonsal, B., and R.G. Lawford (1999), Teleconnections between El Niño and La Niña events and summer extended dry spells on the Canadian prairies, *Int. J. Climatol.*, 19, 1445-1458.

Bonsal, B., A. Shabbar, and K. Higuchi (2001), Impacts of low frequency variability modes on Canadian winter temperature, *Int. J. Climatol.,* 21, 95-108.

Bonsal, B., and A. Shabbar (2008), Impacts of large-scale circulation variability on low streamflows over Canada: a review, *Can. Water. Res. J.*, 33, 137-154.

Burn, D.H. (1994), Hydrological effects of climatic change in west-central Canada, *J. Hydrology*, *160*, 53-70.

Burn, D.H., and M.A. Hag Elnur (2002), Detection of hydrologic trends and variability, *J. Hydrol.*, 255, 107-122.

Burn DH, Fan L, Bell G. 2008. Identification and qualification of streamflow trends on the Canadian Prairies. *Hydrological Sciences* **53**: 538-548.

Chen, Z. and S.E. Grasby (2009), Impact of decadal and century-scale oscillations on hydroclimate trend analyses, *J. Hydrol.*, 365, 122-133.

Comeau, LEL, Pietroniro A, Demuth MN. 2009, Glacier contribution to the North and South Saskatchewan Rivers, *Hydrological Processes* **23**: 2640-2653.

Cryer, J.D. and K.-S. Chan (2008), *Time series analysis with applications in R*, 2nd *ed.*, Springer-Verlag, New York.

Franks SW, Kuczera G. 2002. Flood frequency analysis: evidence and implications of secular climate variability, New South Wales. *Water Resources Research* **38**: 20.1-20.7.

Gan TY. 1998. Hydrocllimatic trends and possible climatic warming in the Canadian Prairies. *Water Resources Research* **34**: 3009-3015.

Gobena AK, Gan TY. 2006 Low-frequency variability in southwestern Canadian streamflow: links with large-scale climate anomalies. *International Journal of Climatology*

Gershunov A, Barnett TP. 1998. Interdecadal modulation of ENSO teleconnections. *Bulletin of the American Meteorological Society* **79**: 2715-2725.

Hamed KH, Rao AR. 1998. A modified Mann-Kendall trend test for autocorrelated data. *Journal of Hydrology* **204**: 219-246.

Harvey KD, Pilon PJ, Yuzyk TR. 1999. Canada's reference hydrometric basin network (RHBN). In: Partnerships in Water Ressources Management. Paper presented at Canadain Water Resources Association (CWRA)'s 51st Annual Conference, June 1999, Halifax, Nova Scotia.

Helsel, D.R., and R.M. Hirsch (2002), *Statistical Methods in Water Resources*, U.S. Geological Society.

Jones PD, Jonsson T, Wheeler D. 1997. Extension to the North Atlantic Oscillation using early instrumental pressure observations from Gibraltar and South-west Iceland. *International Journal of Climato*logy **17**: 1433-1450.

Kendall MG. 1975. *Rank Correlation Methods.* Charles Griffin, London.

Khaliq MN, Ouarda TBMJ, Gachon P, Sushama L, St-Hilaire, A. 2009. Identification of hydrological trends in the presence of serial and cross correlations: a review of selected

methods and their application to annual flow regimes of Canadian rivers. *Journal of Hydrology* **368**: 117-130.
Kiem AS, Franks SW, Kuczera G. 2003. Multi-decadal variability of flood risk. *Geophysical Research Letters* **30**: 7.1-7.4.
Kulkarni A, von Storch H. 1995. Monte Carlo experiments on the effect of serial correlation on the Mann-Kendal test of trend. *Meteorol. Z.* **4**: 82-85.
Kundzewicz ZW, Robson AJ. 2000. *Detecting Trend and Other Changes in Hydrological Data*. World Climate Program-Data and Monitoring. World Meteorological Organization, Geneva (WMO/TD-no. 1013).
Manly, BFJ. 1998. *Randomization, bootstrap and Monte Carlo methods in biology, 2nd ed.* Chapman and Hall, London.
Mann HB. 1945. Non-parametric tests against trend. *Econometrica* **13**: 245-259.
Mantua NJ, Hare SR, Zhang Y, Wallace JM, Francis RC. 1997. A Pacific interdecadal climate oscillation with impacts on salmon production. *Bulletin of the American Meteorological Society* **78**: 1069-1079.
Mantua NJ, Hare SR. 2002. The Pacific Decadal Oscillation. *Journal of Oceanography* **58**: 35-44.
McCabe GJ, Dettinger MJ. 2002. Primary modes and predictability of year-to-year snowpack variations in the western United States from teleconnections with Pacific Ocean climate. *Journal of Hydrometeorology* **3**: 13-25.
McKenney DW, Pedlar JH, Papadopol P, Hutchinson MF. 2006. The development of 1901-2000 historical monthly climate models for Canada and the United States. *Agricultural and Forest Meteorology* **138**: 69-81.
Minobe S. 1997. A 50-70 year climatic oscillation over the North Pacific and North America. *Geophysical Research Letters* **24**: 683-686.
Minobe S. 1999. Resonance in bidecadal and pentadecadal climate oscillations over the North Pacific: role in climatic regime shifts. *Geophysical Research Letters* **26**: 855-858.
Newman M, Compo GP, Alexander MA. 2003. ENSO-forced variability of the Pacific Decadal Oscillation. *Journal of Climate* **16**: 3853-3857.
Newman M. 2007. Interannual to decadal predictability of tropical and North Pacific sea surface temperatures. *Journal of Climate* **20**: 2333-2356.
Pham SV, Leavitt PR, McGowan S, Wissel B, Wassenaar LI. 2009. Spatial and temporal variability of prairie lake hydrology as revealed using stable isotopes of hydrogen and oxygen. *Limnology and Oceanography* **54**: 101-118.
R Development Core Team. 2008. *R: A language and environment for statistical computing.* R Foundation for Statistical Computing, Vienna, Austria. ISBN 3-900051-07-0, URL http://www.R-project.org.
Redmond KT, Koch RW. 1991. Surface climate and streamflow variability in the western United States and their relationship to large-scale circulation indices. *Water Resources Research* **9**: 2381-2399.
Rood, S.B., G.M. Samuelson, J.K. Weber, and K.A. Wywrot (2005), Twentieth-century decline in streamflows from the hydrographic apex of North America, *J. Hydrol.*, 306, 215-233.
Rood, S.B., J. Pan, K.M. Gill, C.G. Franks, G.M. Samuelson, and A. Shepherd (2008), Declining summer flows of Rocky Mountain rivers: changing seasonal hydrology and probable impacts on floodplain forests, *J. Hydrol.*, 349, 397-410.

Ropelewski CF, Jones PD. 1987. An extension of the Tahiti-Darwin Southern Oscillation Index. *Monthly Weather Review* **115**: 2161-2165.

St. Jacques, J.M., and D.J. Sauchyn. (2009) Increasing winter baseflow discharge and mean annual streamflow from possible permafrost thawing in the Northwest Territories, Canada. *Geophysical Research Letters*, 36: L01401, doi:10.1029/2008GL035822.

St. Jacques JM, Sauchyn DJ, Zhao Y. 2010. Northern Rocky Mountain streamflow records: global warming trends, human impacts or natural variability? *Geophysical Research Letters* **37**: L06407, DOI:10.1029/2009GL042045.

Schindler, D.W., and W.F. Donahue (2006), An impending water crisis in Canada's western prairie provinces, *PNAS*, 103, 7210-7216.

Schneider N, Cornuelle BD. 2005. The forcing of the Pacific Decadal Oscillation. *Journal of Climate* **18**: 4355-4373.

Sen PK. 1968. Estimates of the regression coefficient based on Kendall's tau. *Journal of the American Statistical Association* **63**: 1379-1389.

Shabbar, A., and M. Khandekar, (1996), The impact of El Nino-Southern Oscillation on the temperature field over Canada. *Atmosphere-Ocean*, 34, 401-416.

Shabbar, A., B. Bonsal, and M. Khandekar (1997), Canadian precipitation patterns associated with the Southern Oscillation, *J. Clim.*, 10, 3016-3027.

Shabbar, A., and B. Bonsal, (2003), An Assessment of Changes in Winter Cold and Warm Spells over Canada. *Nat. Hazards*, 29, 173-188.

Shabbar, A., and W. Skinner (2004), Summer drought patterns in Canada and the relationship to global sea surface temperatures, *J. Clim.*, 17, 2866-2880.

Smith, L.C., T.M. Pavelsky, G.M. MacDonald, A.I. Shiklomanov and R.B. Lammers (2007), Rising minimum daily flows in northern Eurasian rivers: a growing influence of groundwater in the high-latitude hydrologic cycle, *J. Geophys. Res. 112,* G04S47, doi:10.1029/2006JG000327.

Sokal RR, Rohlf. 1995. *Biometry*, 3rd ed. W.H. Freeman and Company, New York.

Stahl K, Moore RD, McKendry IG. 2006. The role of synoptic-scale circulation in the linkage between large-scale ocean-atmosphere indices and winter surface climate in British Columbia, Canada. *International Journal of Climatology* **26**: 541-560.

Theil H. 1950. A rank-invariant method of linear and polynomial regression analysis, I, II, III. *Nederl. Akad. Wetensch. Proc.* **53**: 386-392, 512-525, 1397-1412.

Wallace JM, Gutzler DS. 1981. Teleconnections in the geopotential height field during the Northern Hemisphere winter. *Monthly Weather Review* **109**: 784-812.

Whitfield PH, Moore RD, Fleming SW, Zawadzki A. 2010. Pacific Decadal Oscillation and the hydroclimatology of Western Canada – reviews and propects. *Canadian Water Resources Journal* **35**: 1-28.

Wise EK. 2010. Spatiotemporal variability of the precipitation dipole transition zone in the western United States. *Geophysical Research Letters* **37**: L07706.

Yu B, Shabbar A, Zwiers FW. 2007. The enhanced PNA-like climate response to Pacific interannual and decadal variability. *Journal of Climate* **20**: 5285-5300.

Yue S, P. Pilon, B. Phinney, and G. Cavadias. 2002a. The influence of autocorrelation on the ability to detect trend in hydrological series, *Hydro. Proc.*, 16, 1807-1829.

Yue S, Pilon P, Cavadias. 2002b. Power of the Mann-Kendall and Spearman's rho tests for detecting monotonic trends in hydrological series. *Journal of Hydrology* **259**: 254-271.

Yue S, Wang C. 2004. The Mann-Kendall test modified by effective sample size to detect trend in serially correlated hydrological series. *Water Resources Management* **18**: 201-218.

Zhang Y, Wallace JM, Iwasaka N. 1996. Is climate variability over the North Pacific a linear response to ENSO? *Journal of Climate* **9**: 1468-1478.

Zhang Y, Wallace JM, Battisti DS. 1997. ENSO-like interdecadal variability: 1900-1993. *Journal of Climate* **10**: 1004-1020.

Zhang, X., K.D. Harvey, W.D. Hogg, and T.R. Yuzyk (2001), Trends in Canadian streamflow, *Water Resour. Res.*, 37, 987-998.

Part III. Appendices

Figure A1. R-code for two-sample, one-sided permutation *t*-tests for PDO's signature

```
negpdo<-read.table("clipboard")    # reading in data
attach(negpdo)
npdo<-negpdo[,1]
pospdo<-read.table("clipboard")
attach(pospdo)
ppdo<-pospdo[,1]

twosam<-function(y1,y2) {n1<-length(y1);n2<-length(y2)      # function declaration t-test
    yb1<-mean(y1); yb2<-mean(y2)
    s1<-var(y1); s2<-var(y2)
    s<- ((n1-1)*s1 + (n2-1)*s2)/(n1 + n2 -2)
    tst <- (yb1-yb2)/ sqrt(s*(1/n1 + 1/n2))
    return(tst)
     }

tstatorig<-twosam(npdo, ppdo)
tstatorig  # tstat original

N <- 10000                          # internal variable declarations
n = length(npdo) + length(ppdo)
cnt = 0
AA = c(npdo, ppdo)
length(AA)
structure=numeric(N)

for (i in 1:N) {                    # permutation test
D=sample(AA,n)
t1=D[1:length(npdo)]; t2=D[(length(npdo) + 1):n]
structure[i] <- twosam(t1,t2)
if (twosam(t1,t2) <=tstatorig) cnt = cnt+1 }

cnt/N                 #  p-level for one-sided test when t < 0
1 - cnt/N             #  use when t > 0; tstat accept if less than 0.05 for a 95% one-tailed
                      #   (upper tail), accept if less than 0.1 for a 90% one-tailed
hist(structure)
```

Table A1. Permutation *t*-test results for the significance of the impact of the winter Pacific Decadal Oscillation (PDO) on Saskatchewan mean daily streamflow. Numbers in bold indicate a significant impact (at the *0.1* level) of the PDO. Red bold denotes a significant negative relationship between the PDO and streamflow, blue bold denotes a significant positive relationship.

Station name	Two-sample *t*-test (-) PDO vs (+) PDO				One-sample *t*-test (+) PDO vs rest				One-sample *t*-test (-) PDO vs rest			
	n_1	n_2	*t*	*p*-value	n_1	n_2	*t*	*p*-value	n_1	n_2	*t*	*p*-value
Rock Creek below Horse Creek	14	15	**1.431**	**0.076**	14	50	**1.709**	**0.039**	15	49	0.264	0.381
Long Creek at Western Crossing	22	22	**1.652**	**0.055**	22	76	**1.401**	**0.072**	22	76	**1.430**	**0.088**
Lyons Creek at International Boundary	19	20	-0.108	0.537	19	63	-0.223	0.392	20	63	0.069	0.458
Lightning Creek near Carnduff	11	6	1.404	0.125	11	25	1.154	0.123	6	30	**1.495**	**0.100**
Antler River near Wauchope	12	10	1.101	0.172	12	33	0.565	0.345	10	35	**1.627**	**0.078**
Notukeu Creek above Admiral Reservoir	11	5	**1.485**	**0.080**	11	24	**1.675**	**0.044**	5	30	0.765	0.219
Swift Current Creek below Rock Creek	12	14	**1.375**	**0.091**	12	43	**1.590**	**0.053**	14	41	0.164	0.426
Bridge Creek at Gull Lake	13	13	0.621	0.274	13	42	0.495	0.327	13	42	0.500	0.301
Cottonwood Creek near Lumsden	11	6	**1.696**	**0.080**	11	25	**1.684**	**0.044**	6	30	1.220	0.124
Stony Creek near Kamsack	11	8	0.784	0.217	11	28	0.721	0.242	8	31	0.230	0.366
Opuntia Lake West Inflow	12	12	0.092	0.468	12	39	-0.619	0.256	12	39	0.812	0.209
Maloneck Creek near Pelly	11	6	0.323	0.369	11	26	0.610	0.281	6	31	-0.106	0.491
Quill Creek near Quill Lake	11	6	0.565	0.302	11	26	1.225	0.114	6	31	-0.302	0.407
Lilian River near Lady Lake	12	8	**2.349**	**0.016**	12	28	**1.741**	**0.037**	8	32	0.963	0.170
Red Deer River near Erwood	12	15	**1.572**	**0.051**	12	44	**1.382**	**0.072**	15	41	0.959	0.179
Overflowing River near Hudson Bay	11	5	0.300	0.363	11	25	**1.715**	**0.040**	5	31	-0.820	0.218
Sturgeon River near Prince Albert	12	8	1.050	0.159	12	30	0.690	0.261	8	34	1.074	0.154
Shell Brook near Shellbrook	12	9	0.716	0.210	12	32	0.678	0.259	9	35	0.578	0.263
Carrot River near Smoky Burn	12	13	**1.574**	**0.067**	12	42	**1.408**	**0.073**	13	41	0.808	0.214
Beaver River near Dorintosh	12	11	**1.421**	**0.084**	12	35	0.995	0.163	11	36	**1.506**	**0.081**
Churchill River above Otter Rapids	12	11	**2.042**	**0.024**	12	34	**1.467**	**0.070**	11	35	**1.477**	**0.077**
Haultain River above Norbert River	11	8	**1.626**	**0.061**	11	28	**1.672**	**0.050**	8	31	1.017	0.156
Gelkie River below Wheeler River	12	9	0.673	0.256	12	31	0.672	0.260	9	34	0.503	0.294
Waterfound River below Theriau Lake	10	5	0.736	0.222	10	24	-0.211	0.411	5	29	1.175	0.126
MacFarlane River at Outlet of Davy Lake	12	9	0.024	0.491	12	30	0.539	0.306	9	33	-0.414	0.345
Fond du Lac River at Black Lake Outlet	11	18	**-1.684**	**0.054**	11	48	-0.966	0.164	18	41	**-1.812**	**0.037**

Table A2. Permutation *t*-test results for the significance of the impact of the Southern Ocean Index (SOI) on Saskatchewan mean daily streamflow. +SOI corresponds to La Niña events and –SOI corresponds to El Niño events. Numbers in bold indicate a significant impact (at the *0.1* level) of the SOI. Red bold denotes a significant positive relationship between the SOI and streamflow, blue bold denotes a significant negative relationship.

Station name	Two-sample *t*-test (+) SOI vs (-) SOI				One-sample *t*-test (+) SOI vs rest				One-sample *t*-test (-) SOI vs rest			
	n_1	n_2	*t*	*p*-value	n_1	n_2	*t*	*p*-value	n_1	n_2	*t*	*p*-value
Rock Creek below Horse Creek	17	21	**2.966**	**0.003**	17	47	**2.735**	**0.006**	21	43	**2.402**	**0.008**
Long Creek at Western Crossing	22	32	**3.725**	**1xe^{-4}**	22	76	**4.185**	**3xe^{-4}**	32	66	**1.665**	**0.041**
Lyons Creek at International Boundary	17	25	-0.058	0.497	17	66	-0.642	0.285	25	58	0.731	0.250
Lightning Creek near Carnduff	8	12	**2.837**	**0.005**	8	28	**4.102**	**2xe^{-4}**	12	24	**1.326**	**0.087**
Antler River near Wauchope	11	15	**2.009**	**0.023**	11	34	**2.764**	**0.008**	15	30	1.097	0.144
Notukeu Creek above Admiral Reservoir	7	12	**1.624**	**0.066**	7	28	**1.764**	**0.051**	12	23	1.176	0.126
Swift Current Creek below Rock Creek	13	16	1.313	0.102	13	42	0.466	0.312	16	39	**1.321**	**0.094**
Bridge Creek at Gull Lake	15	19	**1.549**	**0.066**	15	40	**2.245**	**0.020**	19	36	0.427	0.336
Cottonwood Creek near Lumsden	8	12	**2.886**	**0.005**	8	28	**3.035**	**0.006**	12	24	1.253	0.111
Stony Creek near Kamsack	10	13	0.450	0.352	10	29	0.948	0.180	13	26	-0.176	0.409
Opuntia Lake West Inflow	11	17	0.617	0.274	11	40	1.121	0.133	17	34	-0.239	0.397
Maloneck Creek near Pelly	8	13	-0.408	0.351	8	29	0.310	0.362	13	24	**-1.372**	**0.092**
Quill Creek near Quill Lake	8	13	-0.218	0.427	8	29	0.082	0.440	13	24	-0.555	0.290
Lilian River near Lady Lake	10	14	0.646	0.260	10	30	1.076	0.152	14	26	-0.072	0.462
Red Deer River near Erwood	13	18	-0.274	0.406	13	43	0.330	0.361	18	38	-0.954	0.171
Overflowing River near Hudson Bay	7	13	-0.588	0.309	7	29	-0.367	0.377	13	23	-0.762	0.222
Sturgeon River near Prince Albert	9	14	0.476	0.321	9	33	0.622	0.259	14	28	0.188	0.435
Shell Brook near Shellbrook	10	15	0.349	0.363	10	34	0.346	0.346	15	29	0.249	0.414
Carrot River near Smoky Burn	12	17	0.902	0.185	12	42	1.054	0.150	17	37	0.326	0.381
Beaver River near Dorintosh	11	16	**2.151**	**0.023**	11	36	**3.139**	**0.003**	16	31	0.947	0.178
Churchill River above Otter Rapids	11	16	**1.789**	**0.045**	11	35	**2.553**	**0.010**	16	30	0.622	0.269
Haultain River above Norbert River	9	13	0.456	0.320	9	30	1.047	0.149	13	26	-0.436	0.328
Gelkie River below Wheeler River	10	14	0.634	0.270	10	33	**1.622**	**0.067**	14	29	-0.659	0.261
Waterfound River below Theriau Lake	7	11	0.563	0.285	7	27	0.895	0.182	11	23	0.084	0.467
MacFarlane River at Outlet of Davy Lake	10	14	0.029	0.486	10	32	1.209	0.121	14	28	**-1.485**	**0.073**

Fond du Lac River at Black Lake Outlet	14	18	-0.738	0.231	14	45	-0.717	0.237	18	41	-0.666	0.246

Table A3. Permutation *t*-test results for the significance of the impact of the winter Pacific North American mode (PNA) on Saskatchewan mean daily streamflow. Numbers in bold indicate a significant impact (at the *0.1* level) of the PNA. Red bold denotes a significant negative relationship between the PNA and streamflow, blue bold denotes a significant positive relationship.

Station name	**Two-sample *t*-test (-) PNA vs (+) PNA**				**One-sample *t*-test (+) PNA vs rest**				**One-sample *t*-test (-) PNA vs rest**			
	n_1	n_2	*t*	*p*-value	n_1	n_2	*t*	*p*-value	n_1	n_2	*t*	*p*-value
Rock Creek below Horse Creek	16	10	**2.541**	**0.011**	16	37	**2.656**	**0.004**	10	43	1.194	0.124
Long Creek at Western Crossing	17	15	**2.701**	**0.003**	17	43	**1.799**	**0.028**	15	45	**1.942**	**0.033**
Lyons Creek at International Boundary	17	15	**2.042**	**0.027**	17	43	**1.487**	**0.063**	15	45	**2.461**	**0.014**
Lightning Creek near Carnduff	13	4	-0.196	0.431	13	23	1.129	0.131	4	32	-0.602	0.315
Antler River near Wauchope	14	9	0.569	0.291	14	31	0.709	0.282	9	36	-0.105	0.549
Notukeu Creek above Admiral Reservoir	13	4	1.083	0.145	13	22	**1.808**	**0.035**	4	31	0.398	0.322
Swift Current Creek below Rock Creek	16	12	**3.058**	**0.002**	16	39	**2.561**	**0.004**	12	43	**2.493**	**0.011**
Bridge Creek at Gull Lake	16	9	0.933	0.180	16	32	0.592	0.283	9	46	0.386	0.330
Cottonwood Creek near Lumsden	13	4	**1.917**	**0.082**	13	23	**2.349**	**0.007**	4	32	0.222	0.397
Stony Creek near Kamsack	13	6	0.029	0.402	13	26	-0.944	0.190	6	33	0.611	0.231
Opuntia Lake West Inflow	16	9	1.281	0.120	16	35	1.024	0.154	9	42	**1.399**	**0.095**
Maloneck Creek near Pelly	14	4	-0.810	0.238	14	23	-0.848	0.208	4	33	-0.813	0.213
Quill Creek near Quill Lake	13	4	0.056	0.476	13	24	0.334	0.376	4	33	-0.083	0.514
Lilian River near Lady Lake	14	6	0.570	0.275	14	26	0.448	0.335	6	34	0.541	0.277
Red Deer River near Erwood	16	12	**1.658**	**0.054**	16	40	**1.368**	**0.083**	12	44	0.913	0.187
Overflowing River near Hudson Bay	14	4	-0.382	0.447	14	22	1.128	0.460	4	32	-0.600	0.308
Sturgeon River near Prince Albert	14	6	0.144	0.396	14	28	1.542	0.057	6	36	-0.740	0.245
Shell Brook near Shellbrook	14	8	0.002	0.434	14	30	**1.199**	**0.119**	8	36	-0.817	0.231
Carrot River near Smoky Burn	16	11	**3.030**	**0.004**	16	38	**2.021**	**0.019**	11	43	**2.730**	**0.005**
Beaver River near Dorintosh	15	9	**2.153**	**0.025**	15	32	**1.770**	**0.034**	9	38	1.227	0.116
Churchill River above Otter Rapids	15	9	**1.700**	**0.049**	15	31	**1.504**	**0.065**	9	37	0.423	0.325
Haultain River above Norbert River	13	6	0.346	0.359	13	25	**1.846**	**0.034**	6	33	-0.590	0.282
Gelkie River below Wheeler River	14	7	0.668	0.250	14	29	1.121	0.136	7	36	0.222	0.391

Waterfound River below Theriau Lake	12	4	-0.235	0.427	12	22	0.299	0.383	4	30	-0.468	0.328
MacFarlane River at Outlet of Davy Lake	13	7	**-1.456**	**0.081**	13	29	0.093	0.476	7	35	**-1.867**	**0.027**
Fond du Lac River at Black Lake Outlet	15	15	**-2.191**	**0.020**	15	44	-0.810	0.205	15	44	**-3.156**	**0.001**

Table A4. Permutation *t*-test results for the significance of the impact of the winter Arctic Oscillation (AO) on Saskatchewan mean daily streamflow. Numbers in bold indicate a significant impact (at the *0.1* level) of the AO. Red bold denotes a significant negative relationship between the AO and streamflow, blue bold denotes a significant positive relationship.

Station name	Two-sample *t*-test (-) AO vs (+) AO				One-sample *t*-test (+) AO vs rest				One-sample *t*-test (-) AO vs rest			
	n_1	n_2	*t*	*p*-value	n_1	n_2	*t*	*p*-value	n_1	n_2	*t*	*p*-value
Rock Creek below Horse Creek	15	12	0.901	0.193	15	49	0.785	0.224	12	52	0.644	0.259
Long Creek at Western Crossing	20	22	-0.226	0.413	20	78	-0.754	0.224	22	76	0.346	0.367
Lyons Creek at International Boundary	16	20	**1.432**	**0.078**	16	67	**1.403**	**0.070**	20	63	0.536	0.290
Lightning Creek near Carnduff	12	6	-0.179	0.490	12	24	-0.524	0.302	6	30	0.028	0.407
Antler River near Wauchope	13	9	0.087	0.449	13	32	-1.014	0.183	9	36	0.968	0.184
Notukeu Creek above Admiral Reservoir	12	6	-0.964	0.170	12	23	-1.276	0.105	6	29	-0.625	0.274
Swift Current Creek below Rock Creek	13	13	**1.952**	**0.029**	13	42	0.898	0.190	13	42	**2.212**	**0.020**
Bridge Creek at Gull Lake	14	11	**1.655**	**0.056**	14	41	**1.557**	**0.056**	11	44	0.728	0.229
Cottonwood Creek near Lumsden	12	6	0.234	0.373	12	24	0.314	0.393	6	30	0.132	0.405
Stony Creek near Kamsack	13	6	0.222	0.373	13	26	-0.426	0.331	6	33	0.640	0.220
Opuntia Lake West Inflow	13	11	**1.613**	**0.065**	13	38	0.799	0.228	11	40	**2.367**	**0.020**
Maloneck Creek near Pelly	12	7	1.092	0.144	12	25	-0.121	0.445	7	30	**1.943**	**0.039**
Quill Creek near Quill Lake	13	6	0.710	0.243	13	24	-1.020	0.158	6	31	**1.834**	**0.049**
Lilian River near Lady Lake	13	7	0.449	0.322	13	27	-0.903	0.189	7	33	1.368	0.103
Red Deer River near Erwood	13	13	1.104	0.144	13	43	0.206	0.450	13	43	**1.658**	**0.064**
Overflowing River near Hudson Bay	12	7	1.334	0.112	12	24	0.352	0.377	7	29	**1.758**	**0.056**
Sturgeon River near Prince Albert	13	8	0.416	0.330	13	29	0.427	0.332	8	34	0.935	0.180
Shell Brook near Shellbrook	13	9	0.429	0.334	13	31	-0.718	0.236	9	35	1.292	0.106
Carrot River near Smoky Burn	13	13	**1.819**	**0.039**	13	41	0.526	0.317	13	41	**2.844**	**0.006**
Beaver River near Dorintosh	13	9	0.950	0.179	13	34	0.486	0.330	9	38	0.944	0.179
Churchill River above Otter Rapids	13	9	1.078	0.142	13	33	0.289	0.601	9	37	1.258	0.111

Haultain River above Norbert River	13	7	0.303	0.386	13	26	-0.267	0.390	7	32	0.576	0.275
Gelkie River below Wheeler River	13	8	-0.084	0.474	13	30	-0.509	0.303	8	35	0.227	0.395
Waterfound River below Theriau Lake	12	5	0.205	0.406	12	22	0.492	0.313	5	29	-0.039	0.491
MacFarlane River at Outlet of Davy Lake	13	8	-0.487	0.350	13	29	-1.195	0.118	8	34	0.214	0.404
Fond du Lac River at Black Lake Outlet	13	15	-1.084	0.146	13	46	**-1.433**	**0.081**	15	44	-0.417	0.348